

Arithmetic and geometry of a K3 surface emerging from virtual corrections to Drell–Yan scattering

Marco Besier,^{a,b} Dino Festi,^a Michael Harrison,^{c,d} Bartosz Naskręcki^e

^a*Institut für Mathematik, Johannes Gutenberg-Universität Mainz, 55099 Mainz, Germany*

^b*PRISMA Cluster of Excellence, Institut für Physik, Johannes Gutenberg-Universität Mainz, 55099 Mainz, Germany*

^c*School of Mathematical Sciences, University of Nottingham, NG7 2RD Nottingham, United Kingdom*

^d*MAGMA Computational Algebra Group, School of Mathematics and Statistics, University of Sydney, NSW 2006, Australia*

^e*Faculty of Mathematics and Computer Science, Adam Mickiewicz University, 61-614 Poznań, Poland*

E-mail: mbesie01@uni-mainz.de, dfesti@uni-mainz.de, mch1728@gmail.com, bartnas@amu.edu.pl

ABSTRACT: We study a K3 surface, which appears in the two-loop mixed electroweak-quantum chromodynamic virtual corrections to Drell–Yan scattering. A detailed analysis of the geometric Picard lattice is presented, computing its rank and discriminant in two independent ways: first using explicit divisors on the surface and then using an explicit elliptic fibration. We also study in detail the elliptic fibrations of the surface and use them to provide an explicit Shioda–Inose structure. Moreover, we point out the physical relevance of our results.

Contents

1	Introduction	2
2	Physical background and motivation	3
2.1	Particle physics and Drell–Yan scattering	3
2.2	Feynman integrals via differential equations	5
2.3	The problem of rationalising square roots	7
3	The Drell–Yan K3 surface and its Picard lattice	8
3.1	The Drell–Yan K3 surface	8
3.2	Computing the geometric Picard lattice	9
3.3	An application: computation of the Brauer group	12
4	Elliptic fibrations on the surface	13
4.1	Background on elliptic fibrations	13
4.2	General method and results for the Drell–Yan surface	14
4.3	First elliptic fibration	17
4.4	Second elliptic fibration	18
4.5	Third elliptic fibration	19
5	Computation of the Shioda–Inose structure	21
5.1	Shioda–Inose structure on the Drell–Yan K3 surface	21
5.2	Supersingular reduction	26
6	Computing the Picard lattice via elliptic fibrations	27
6.1	A different proof	28
6.1.1	The rank	28
6.1.2	Height pairing computations	29
6.1.3	Discriminant formula	29
6.1.4	Néron–Severi group basis	30

1 Introduction

Given the advancing precision of measurements carried out at modern particle colliders, equally precise theoretical predictions are required. To perform these computations, one has to solve the most complicated Feynman integrals. It turns out that the rationality problem for hypersurfaces often marks an essential step in the calculation of these integrals [11, 17, 27, 38, 43, 78]. As a consequence, methods from algebraic and arithmetic geometry are becoming increasingly important for theoretical particle physics. In this paper, we study the rationality problem for a hypersurface derived from Feynman integrals contributing to the mixed electroweak-quantum chromodynamics corrections to Drell–Yan scattering.

In most cases, the preferred method of solving Feynman integrals is to solve them in terms of multiple polylogarithms (MPLs), as these functions are well understood and implemented for numerical evaluation [6, 76]. In an attempt to compute the above mentioned Drell–Yan corrections in terms of MPLs, one would ideally want to find a rational parametrisation of the projective surface given by

$$X_{DY}: w^2 = 4xy^2z(x-z)^2 + (x+y)^2(xy+z^2)^2 \quad (1.1)$$

in the weighted projective space $\mathbb{P}(1, 1, 1, 3)$ over \mathbb{Q} with coordinates x, y, z, w of weights 1, 1, 1, 3, respectively.

Remark 1.1. For the reader who never encountered weighted projective spaces before, these can be regarded as a generalisation of projective spaces by artificially changing the *weight* of the coordinates of the space and hence changing the condition for a polynomial to be homogeneous. For example, in a space in which the coordinates x_0 and x_1 have weight 1 and 2, respectively, the polynomial $x_0^2 - x_1$ is homogeneous of degree 2. A classical reference for this topic is [31].

As a first result, we prove the following theorem.

Theorem 1.2. *The surface X_{DY} defined in (1.1) is birationally equivalent to a K3 surface. Therefore, it does not admit a rational parametrisation.*

Let us recall the definition of a K3 surface.

Definition 1.3. Let Y be a smooth, projective, geometrically integral surface over a field k . We say that Y is a K3 surface if it has first cohomology class $H^1(Y, \mathcal{O}_Y) = 0$ and canonical divisor $K_Y = 0$.

Remark 1.4. Alternatively, Definition 1.3 is equivalent to saying that a K3 surface is a simply connected Calabi–Yau manifold of dimension 2, i.e., a smooth, simply connected surface admitting a nowhere vanishing holomorphic 2-form.

As noted in [35], also the two-loop virtual corrections to Bhabha scattering give rise to a K3 surface, and so one might ask if the surfaces arising from the Bhabha and the Drell–Yan scatterings are related, or even the same. We prove that this is not the case, by showing that the Picard lattices of the two surfaces are not isometric.

Theorem 1.5. *Let X_{DY} be the surface defined by (1.1), and let B be the surface defined in [35]. Then X_{DY} is not birationally equivalent to B , nor to any of the deformations of B considered in [35].*

Although the surface X_{DY} is not parametrisable by rational functions and it is not isomorphic to the surface arising from Bhabha scattering, something can still be done to solve the integrals: for example, one can leave the non-rationalisable square root untouched and express the result in terms of MPLs with algebraic arguments [43].

Alternatively, one may hope to solve the integrals in terms of elliptic multiple polylogarithms (eMPLs). This approach has recently led to a very compact result for the master integrals of the two-loop Bhabha corrections [73]. To perform this computation, one needs to use elliptic fibrations on the associated K3 surface. Therefore, we expect that elliptic fibrations on X_{DY} will enable physicists to compute the result of the Drell–Yan master integrals in terms of eMPLs. For this reason, we present a computational method to find many elliptic fibrations of X_{DY} in Section 4, and explicitly describe three of them.

In order to prove Theorems 1.2 and 1.5, it is enough to consider a smooth model S_{DY} (cf. Definition 3.2) of X_{DY} and study its (geometric) Picard lattice. Finding elliptic fibrations on X_{DY} is equivalent to finding elliptic fibrations on S_{DY} . The methods used are not new, but this paper represents an attempt to establish an algorithmic and concrete approach to these problems. In this way, we hope to help all the physicists, and—more generally—the non-specialists in algebraic geometry in solving these problems that often represent a severe obstacle in their research.

We proceed as follows: a physical motivation and an introduction to the problem are given in Section 2. In Section 3 and 6 we compute the Picard lattice of S_{DY} in two different ways: exhibiting explicit divisors, and using an elliptic fibration, respectively. Furthermore, we use the computations in Section 3 to deduce some information about the Brauer group of S_{DY} (Subsection 3.3). The computation of elliptic fibrations of S_{DY} is provided in Section 4. Besides being useful for (re-)computing the geometric Picard lattice of the K3 surface, these elliptic fibrations allow us to explicitly describe a Shioda–Inose structure of S_{DY} , which is done in Section 5. In consequence, we also compute the number of points on the reduction of the surface S_{DY} to positive characteristic.

Some proofs in this paper are aided by explicit computations using the software package `Magma` (cf. [15]). This is explicitly stated in the proofs where such computations are needed. The `Magma` code used in the proofs can be found in the ancillary file [10] available online.

2 Physical background and motivation

2.1 Particle physics and Drell–Yan scattering

In physics, all possible interactions of matter can be reduced to four fundamental forces. On the one hand, one has gravitational and electromagnetic interactions, whose effects we experience in our everyday life. On the other hand, one has the strong and the weak interactions that produce forces at subatomic distances.

While the gravitational force is successfully described by Einstein’s general theory of relativity, the strong, weak, and electromagnetic interactions are described by the Standard Model (SM) of particle physics—a term which has become a synonym for a quantum field theory (QFT) based on the gauge group $SU(3) \times SU(2) \times U(1)$. The groups $SU(3)$, $SU(2)$, and $U(1)$ constitute the gauge groups for the strong, weak, and electromagnetic force, respectively. Accordingly, the SM contains three coupling constants g_1, g_2 and g_3 —one for each of the three fundamental interactions described by the SM. The respective QFTs that are used for the theoretical description of these interactions are quantum chromodynamics (QCD) and electroweak (EW) theory, the latter being the unification of weak theory and quantum electrodynamics (QED).

To test the validity of the SM, experimental physicists investigate scattering processes, i.e., collisions of particles generated by electron or proton beams. In the search for new elementary particles, these collisions are performed at very high energies in huge particle colliders, the world’s most famous being the Large Hadron Collider (LHC) at the CERN laboratory in Geneva, Switzerland.

In the regime of high energies, the aforementioned coupling constants g_1, g_2, g_3 of the SM are very small and perturbation theory, i.e., regarding physical observables as power series in the coupling constants, turns out to be a valuable tool to obtain theoretical predictions. For this reason, perturbative QFT is often referred to as theoretical high energy particle physics.

One of the most critical scattering processes studied at the LHC is the Drell–Yan production of Z and W bosons [32]. Due to their clean experimental signature, Drell–Yan processes can be measured with comparatively small experimental uncertainty, allowing for very precise tests of the SM and numerous applications in other scattering experiments. For instance, the Drell–Yan mechanism provides valuable information about the parton distribution functions, which are essential for theoretical studies of processes at virtually any hadron collider around the globe. Because of the sharp experimental signal, Drell–Yan scattering is also used for detector calibration of the LHC itself and for the determination of its collider luminosity. Finally, Drell–Yan processes are crucial in searches for physics beyond the SM involving new, yet to discover elementary particles such as Z' and W' that originate from Grand Unified Theory (GUT) extensions of the SM. For all these reasons, an accurate and reliable experimental setup as well as very precise theoretical descriptions of the Drell–Yan mechanism are of vital importance for contemporary particle physics at the LHC.

Latest theoretical predictions for this scattering process are in reasonable agreement with the experimental data. Nevertheless, even more precise computations are indispensable. To improve theoretical accuracy, one needs to take into account higher-order perturbative corrections. Currently, the theoretical description of Drell–Yan processes includes QCD corrections of second order [1, 2, 40, 56] as well as EW corrections up to first order of the respective perturbation series [7, 79]. Second-order corrections to the Drell–Yan process in QED with massive fermions were recently considered in [12]. Moreover, there are some other significant second-order perturbative contributions, whose full analytic structure was also studied only recently, one of the most difficult being the mixed EW-QCD corrections

[13, 43, 77]. It is of maximum importance to get a solid understanding of these newly discovered contributions to match future experimental requirements, especially in view of run III of the LHC, starting in 2021.

2.2 Feynman integrals via differential equations

The crux of a typical computation in theoretical particle physics is the fact that, in order to determine the sought after coefficients of the relevant perturbation series, one has to solve certain integrals, often referred to as Feynman integrals. For this reason, these integrals may be regarded as the building blocks for the study of any scattering process in perturbative QFT. Unfortunately, Feynman integrals are usually extremely difficult to compute and often even divergent under the assumption of a four-dimensional space-time. In order to deal with these divergences, one needs to introduce a regulator. While there are several ways to do this, the method of dimensional regularisation has become standard. Roughly speaking, one replaces a four-dimensional integral by an integral in D dimensions, where D depends on a small regularisation parameter $\epsilon > 0$. In practice, one usually assumes $D = 4 - 2\epsilon$ such that the “physical limit” is recovered when putting $\epsilon \rightarrow 0$.

Despite the extreme complexity of Feynman integral calculations, the last decades have witnessed an impressive advancement in the identification of mathematical tools that can be put into action to perform these complicated computations. One method that has proven itself to be spectacularly successful is the utilisation of differential equations, satisfied by the Feynman integrals: solving a system of differential equations for a given set of Feynman integrals, one can obtain the final result while circumventing the need to perform the original integrations [8, 39, 50, 66]. These days, solving Feynman integrals via differential equations has become one of the standard ways to compute higher-order corrections for scattering processes.

Let us see how this method works in practice through a simple example. Therefore, consider the following two Feynman integrals that are needed for a certain first-order correction in QED:

$$\begin{aligned} I_1 &= (m^2)^{2-\frac{D}{2}} \int \frac{d^D k}{i\pi^{\frac{D}{2}}} \frac{1}{[m^2 - k^2]^2} \\ I_2 &= (m^2)^{3-\frac{D}{2}} \int \frac{d^D k}{i\pi^{\frac{D}{2}}} \frac{1}{[m^2 - k^2]^2 [m^2 - (k-p)^2]} \end{aligned} \tag{2.1}$$

In the above, m denotes a real constant referring to a particle mass, whereas p should be viewed as a variable referring to a particle momentum that may vary depending on the experimental setup. In this sense, one may view I_1 and I_2 as functions depending on p . Working in dimensional regularisation, we assume $D = 4 - 2\epsilon$. The two integrals I_1 and I_2 represent a particular choice of what is called a basis of master integrals. More precisely, this means that all Feynman integrals that are relevant for computing the sought after perturbative correction can be reduced to I_1 and I_2 . It is an important fact that the choice of a basis of master integrals for a given perturbative correction is not unique. As we will see below, for practical purposes, there are some choices of master integrals that are more appropriate than others.

Viewing I_1 and I_2 as functions of $x := p^2/m^2$, we find the following differential equation for $\vec{I} = (I_1, I_2)^T$:

$$\frac{d}{dx}\vec{I} = \begin{pmatrix} 0 & 0 \\ \frac{\epsilon}{4x} - \frac{\epsilon}{4(x-4)} & -\frac{1}{2x} - \frac{1+2\epsilon}{2(x-4)} \end{pmatrix} \vec{I}. \quad (2.2)$$

Notice that all entries of the matrix on the right-hand side are rational functions of x .

Next, one tries to find what is called an ϵ -*decoupled basis* of master integrals [44, 51]. Recall that we have some freedom in choosing a basis of master integrals for the perturbative correction at hand. More precisely, it would be beneficial to bring the differential equation into a form, where the only explicit ϵ -dependence is through a prefactor on the right-hand side. To achieve this, we divide I_1 and I_2 by their maximal cuts [14, 28, 37, 41, 54, 55, 64]. Changing our basis of master integrals from I_1 and I_2 to

$$J_1 = 2\epsilon I_1, \quad J_2 = 2\epsilon\sqrt{-x(4-x)}I_2, \quad (2.3)$$

the differential equation (2.2) becomes

$$\frac{d}{dx}\vec{J} = \epsilon \begin{pmatrix} 0 & 0 \\ -\frac{1}{\sqrt{-x(4-x)}} & -\frac{1}{x-4} \end{pmatrix} \vec{J}. \quad (2.4)$$

The differential equation is now given in what physicists call the ϵ -*decoupled form*. Notice that, in order to obtain the ϵ -decoupled form, we had to pay the price of introducing a square root in the matrix entries. We may, however, change variables [4] setting

$$x = -\frac{(1-t)^2}{t}. \quad (2.5)$$

This substitution turns the matrix entries into rational functions of the new variable t . Indeed, we find

$$\frac{d}{dt}\vec{J} = \epsilon \begin{pmatrix} 0 & 0 \\ -\frac{1}{t} & \frac{1}{t} - \frac{2}{t+1} \end{pmatrix} \vec{J}. \quad (2.6)$$

Having the differential equation in ϵ -decoupled form and all matrix entries given as rational functions, it is straightforward to write down the final result for J_1 and J_2 in terms of MPLs.

Though comparatively simple, the above considerations provide a typical example for the calculation of a given basis of master integrals. While most steps can naturally be carried over to more complicated physical use cases, it turns out that one of the most demanding tasks is to find a change of variables like (2.5) that transforms the square roots appearing in the matrix entries into rational functions. In the case of more ambitious perturbative corrections, this *rationalisation problem* often marks an insurmountable difficulty for most practitioners.

2.3 The problem of rationalising square roots

Besides the success of momentum twistor variables [17, 25, 38, 46], it was only recently that a systematic way to approach this problem was brought from mathematics to the physics community [11]. This systematic approach relies on the fact that square roots can readily be associated with algebraic hypersurfaces. For instance, a reasonable choice of a hypersurface associated with the above square root is the algebraic curve

$$\mathcal{C} : y^2 + x(4 - x) = 0. \quad (2.7)$$

Notice that, if we are able to find a rational parametrisation of this curve, then we can use this parametrisation to turn the square root $\sqrt{-x(4 - x)}$ into a rational function of t . Indeed, a possible parametrisation for \mathcal{C} is

$$x(t) = -\frac{(1 - t)^2}{t}, \quad y(t) = \frac{1 - t^2}{t}, \quad (2.8)$$

corresponding to the change of variables given in (2.5).

In the above example, we are dealing with a plane conic curve. Thus, finding a rational parametrisation is an easy task. Computing more sophisticated perturbative corrections, however, one is likely to encounter square roots which are much more difficult to turn into rational functions. For a long time, it was, for example, not clear to physicists how to find a change of variables that transforms the square root

$$\sqrt{\frac{(x + y)(1 + xy)}{x + y - 4xy + x^2y + xy^2}} \quad (2.9)$$

into a rational function. This square root shows up in the context of second-order corrections to Bhabha scattering [45] and was recently proven to be non-rationalisable [35].

Indeed, the hypersurface associated with this square root is birational to a double cover of \mathbb{P}^2 ramified above a sextic curve with ADE singularities only. Therefore, this hypersurface is birational to a K3 surface, and a change of variables turning (2.9) into a rational function would imply the existence of a rational parametrisation of the associated K3 surface, which is impossible since K3 surfaces are not rational. Thus, there is no rational change of variables that would turn (2.9) into a rational function.

Besides this particular example involving a K3 surface, a lot of perturbative corrections over the last couple of years led to square roots associated with elliptic curves. Feynman integrals, whose computation involves this kind of non-rationalisable square roots can, in general, no longer be solved in terms of MPLs [53].

It was only recently that the notion of eMPLs was introduced [21, 23], which finally enabled physicists to find analytic solutions to perturbative corrections that were previously out of reach. Following this line of reasoning, one could naively think that one has to come up with a ‘‘K3 type version’’ of MPLs in order to solve differential equations involving square roots associated with K3 surfaces.

It turned out, however, that even in this more complicated case, one is still able to use eMPLs, if the K3 surface is elliptically fibered. For this very reason, physicists were finally

able to compute the aforementioned Bhabha correction analytically in terms of eMPLs [73]. This shows that the study of elliptic fibrations is crucial for higher-order corrections in perturbative QFT—particularly because we observe that an increasing number of recent perturbative corrections turn out to involve K3 surfaces [16, 18, 22, 24].

Let us now come back to the mixed EW-QCD corrections to Drell–Yan scattering. Trying to compute the relevant master integrals, one encounters the following square root [13]:

$$\sqrt{4xy^2(1+x)^2 + (x(1+y)^2 + y(1+x)^2) \cdot (x(1-y)^2 + y(1-x)^2)}. \quad (2.10)$$

The physical motivation for a mathematical investigation of this square root is threefold. First, one wants to know whether one can find a change of variables that turns (2.10) into a rational function. In the upcoming section of this paper, we prove that this is *not* the case by showing that the hypersurface associated with (2.10) is birational to a K3 surface.

Secondly, a physicist would hope that one is at least able to find a change of variables that relates the K3 appearing in Drell–Yan scattering with a K3 surface that is already well-studied, e.g., the K3 appearing in the context of Bhabha scattering. In such a case one might be able to reuse some known techniques from Bhabha scattering in the context of the Drell–Yan corrections. Mathematically, this is asking for a birational map between the two K3 surfaces. By providing a detailed study of the Picard lattice structure of the K3 associated with (2.10), we prove that such a birational map does *not* exist (cf. Corollary 3.9).

Lastly, as already mentioned in the introduction, we expect the use of elliptic fibrations of the above K3 to be a key ingredient when trying to obtain the analytic result for the Drell–Yan correction in terms of eMPLs. For this reason, in Section 4 we provide a thorough study of the elliptic fibrations relevant to Drell–Yan scattering.

3 The Drell–Yan K3 surface and its Picard lattice

Section 2 left us with some questions about the square root (2.10): is it possible to find a change of variables turning it into a rational function? Is it possible to find a change of variables such that the surface associated with it is isomorphic to the K3 surface emerging from the Bhabha scattering? In this section, we are going to show that both questions have a negative answer, hence proving Theorems 1.2 and 1.5 (see corollaries 3.3 and 3.9, respectively).

3.1 The Drell–Yan K3 surface

If $f(X, Y)$ is a polynomial of even degree $2d$, then there is a natural way to associate a surface with the square root $\sqrt{f(X, Y)}$. Let $\tilde{f}(x, y, z)$ be the homogenisation of f via the substitution $X := x/z$ and $Y := y/z$. If $u = \sqrt{f(X, Y)}$, then $uz^d = \sqrt{\tilde{f}(x, y, z)}$. Substituting uz^d with w and squaring both sides, we get the equation

$$w^2 = \tilde{f}(x, y, z),$$

which defines a surface in the weighted projective space $\mathbb{P}(1, 1, 1, d)$ with coordinates x, y, z , and w , respectively.

Using the procedure above and rearranging the summands of the polynomial, one can easily see that (2.10) is associated with the surface X_{DY} defined by

$$w^2 = 4xy^2z(x-z)^2 + (x+y)^2(xy+z^2)^2 \quad (3.1)$$

in the weighted projective space $\mathbb{P} := \mathbb{P}(1, 1, 1, 3)$ with coordinates x, y, z, w . We define the map $\pi: X_{DY} \rightarrow \mathbb{P}^2$ by $\pi: (x : y : z : w) \rightarrow (x : y : z)$.

Lemma 3.1. *The surface X_{DY} has five singular points, namely:*

- $P_1 := (1 : 1 : -1 : 0)$, of type A_1 ;
- $P_2 := (0 : 0 : 1 : 0)$, of type A_2 ;
- $P_3 := (1 : -1 : 1 : 0)$, of type A_3 ;
- $P_4 := (1 : 0 : 0 : 0)$, of type A_4 ;
- $P_5 := (0 : 1 : 0 : 0)$, of type A_4 .

Proof. The surface X_{DY} is a double cover of \mathbb{P}^2 branched above the plane curve $B: f = 0$. Therefore, the singularities of X_{DY} come from the singularities of B , which can easily be found by direct computations. In order to find the type of singularity, it is enough to consider a double cover of the resolution of the singularities of B (see, e.g., II, Sec. 8 and III, Sec. 7 of [5]). \square

Definition 3.2. Let $S := S_{DY}$ be the desingularisation of X_{DY} .

Proposition 3.3. *S is a K3 surface.*

Proof. This follows from the theory of invariants of double covers with simple singularities as described in V, Sec. 22 of [5]. The map π gives X_{DY} the structure of a double cover of \mathbb{P}^2 , hence $H^1(X_{DY}, \mathcal{O}_X) = 0$. It ramifies above the plane curve defined by $4xy^2z(x-z)^2 + (x+y)^2(xy+z^2)^2 = 0$, which is a sextic, and therefore $K_X = 0$.

Because S is the desingularisation of X , it is smooth. We also have that $H^1(S, \mathcal{O}_S) = 0$ and that the canonical divisor is unchanged by the resolutions, since all the singular points are of A-type (DuVal singularities). Therefore, $K_S = 0$. It follows that S is a K3 surface. \square

Corollary 3.4. *The square root (2.10) is not rationalisable by a rational change of variables.*

Proof. Rationalising the square root (2.10) by a rational change of variables is equivalent to finding a rational parametrisation of X_{DY} , i.e., proving that X_{DY} is a rational surface. The desingularisation S of X_{DY} is a K3 surface, hence not a rational surface. This implies that X_{DY} is not a rational surface either. \square

3.2 Computing the geometric Picard lattice

In this subsection, we are going to compute the Picard lattice of $S = S_{DY}$. In doing so we follow the method explained in [34].

Proposition 3.5. *The surface S has geometric Picard number $\rho(\overline{S}) \leq 19$.*

Proof. We use van Luijk’s method with Kloosterman’s refinement, cf. [49, 75]. By Weil and Artin–Tate conjectures (both proven true for K3 surfaces over finite fields, cf. [30] for the proof of the Weil conjectures, and see for example [3, 26] for the proof of the Tate conjecture for K3 surfaces over finite fields of characteristic $p \geq 5$), we have that for a K3 surface over a finite field with q elements:

- the Picard number equals the number of roots of the Weil polynomial of the surface which is equal to q ,
- the discriminant of the Picard lattice is equal, up to squares, to the product

$$q \cdot \prod_{i=1+\rho(X)}^{22} (1 - \alpha_i/q) .$$

After checking that 31 and 71 are prime of good reduction for S , we use **Magma** to compute the Weil polynomial of the reduction S_q of S over the finite field \mathbb{F}_q and we found the following results:

- $\rho(\overline{S_{31}}) = 20$ and $|\text{disc Pic } \overline{S_{31}}| \equiv 3 \pmod{(\mathbb{Q}^*)^2}$;
- $\rho(\overline{S_{71}}) = 20$ and $|\text{disc Pic } \overline{S_{71}}| \equiv 35 \pmod{(\mathbb{Q}^*)^2}$.

Recall that the Picard lattice of a K3 surface over a number field injects into the Picard lattice of its reduction modulo a prime via a torsion-free-cokernel injection. Then, if we assume that $\rho(\overline{S}) = 20$, it follows that $\text{disc Pic } \overline{S} = \text{disc Pic } \overline{S_{31}} = \text{disc Pic } \overline{S_{71}}$ which is impossible, as the discriminants of $\text{Pic } \overline{S_{31}}$ and $\text{Pic } \overline{S_{71}}$ are not equivalent up to squares and therefore cannot be equal. \square

We show that the geometric Picard number $\rho(\overline{S})$ is exactly 19 by considering the sublattice generated by the following divisors. As S is the resolution of X_{DY} , on S we have the exceptional divisors lying above the singular points of X_{DY} , namely:

- $E_{1,1}$ above the point P_1 ;
- $E_{2,-1}$ and $E_{2,1}$ above P_2 ;
- $E_{3,-1}$, $E_{3,0}$, and $E_{3,-1}$ above P_3 ;
- $E_{i,-2}$, $E_{i,-1}$, $E_{i,1}$, and $E_{i,2}$ above P_i , for $i = 4, 5$.

Furthermore, consider the following nine divisors of X_{DY} .

$$\begin{aligned} L'_1: & x = 0, \quad w - yz^2 \\ L'_2: & x - z = 0, \quad w - z(y + z)^2 = 0 \\ L'_3: & y + \frac{3 - \sqrt{5}}{2}z, \quad w + \frac{3 - \sqrt{5}}{2}z(x^2 - xz + z^2) = 0 \\ L'_4: & y + \frac{3 + \sqrt{5}}{2}z, \quad w + \frac{3 + \sqrt{5}}{2}z(x^2 - xz + z^2) = 0 \\ L'_5: & y = 0, \quad w - xz^2 = 0 \\ L'_6: & y + z = 0, \quad w - z(x - z)(x + z) = 0 \\ L'_7: & z = 0, \quad w - xy(x + y) = 0 \end{aligned}$$

$$\begin{aligned}
C'_1: x^2 + \frac{-1 + \sqrt{5}}{2}(xy + xz) + yz &= 0, \\
xy^2 + \frac{5 + \sqrt{5}}{2}xyz + \frac{5 + 3\sqrt{5}}{2}y^2z + \frac{3 + \sqrt{5}}{2}xz^2 + \frac{5 + 3\sqrt{5}}{2}yz^2 + \frac{3 + \sqrt{5}}{2}w &= 0 \\
C'_2: x^2 + \frac{-1 - \sqrt{5}}{2}(xy + xz) + yz &= 0, \\
xy^2 + \frac{5 - \sqrt{5}}{2}xyz + \frac{5 - 3\sqrt{5}}{2}y^2z + \frac{3 - \sqrt{5}}{2}xz^2 + \frac{5 - 3\sqrt{5}}{2}yz^2 + \frac{3 - \sqrt{5}}{2}w &= 0
\end{aligned}$$

For $i = 1, \dots, 7$ and $j = 1, 2$, we define L_i and C_j to be the strict transform of L'_i and C'_j , respectively, on S . Finally, let H' denote the hyperplane section on X_{DY} ; we define H to be the pullback of H' on S . Let Σ be the set of the 24 divisors of S defined so far, and let $\Lambda \subseteq \text{Pic } S$ be the sublattice of $\text{Pic } S$ generated by the classes of the elements in Σ .

Proposition 3.6. *The sublattice Λ has rank 19, discriminant $2^3 \cdot 3$ and discriminant group isomorphic to $\mathbb{Z}/2\mathbb{Z} \times \mathbb{Z}/2\mathbb{Z} \times \mathbb{Z}/6\mathbb{Z}$.*

Proof. The intersection matrix of these divisors has been computed using a built-in **Magma** function to determine the intersection numbers between the strict transforms of surface divisors and the exceptional divisors and a custom function for the local intersection numbers between the strict transforms over the singular points. This function can be found in the accompanying **Magma** file [10]. See also Remark 4.6. \square

Remark 3.7. Proposition 3.6 can be proven also in a different way, less explicit but also involving fewer **Magma** coding skills. Indeed, notice the following remarks.

- $H^2 = 2$; for every i, j , $H.E_{i,j} = 0$; for every i , $H.L_i = 1$; for every j , $H.C_j = 2$.
- For every i, j , $C_j^2 = L_i^2 = -2$. The intersection numbers $L_i.L_j$, $L_i.C_j$, $C_i.C_j$ can be explicitly computed as we have the explicit defining equations.
- The intersection numbers of the exceptional divisors are completely determined by the type of singularity.
- A few intersection numbers between the exceptional divisors and the divisors L_i, C_j can be determined by an *ad hoc* labeling of the exceptional divisors.

These remarks still leave some intersection numbers undetermined. These undetermined numbers can either be 1 or 0. Using a computer, one can go through all the combinations and find that only one combination satisfies the condition $\text{rk } \Lambda \leq 20$. This combination returns the quantities in the statement. These computations can be found in the accompanying **Magma** file.

Theorem 3.8. $\text{Pic } \bar{S} = \Lambda$.

Proof. In this proof, we denote $\text{Pic } \bar{S}$ by simply P . From Propositions 3.5 and 3.6 it immediately follows that P has rank 19 and hence Λ is a finite-index sublattice of P . As the discriminant of Λ is $24 = 2^3 \cdot 3$, the index $[P : \Lambda]$ is either 1 or 2.

For a contradiction, assume $[P : \Lambda] = 2$ and let $\iota : \Lambda \hookrightarrow P$ be the inclusion map. Then the induced map $\iota_2 : \Lambda/2\Lambda \rightarrow P/2P$ has exactly one non-zero element in its kernel $\ker \iota_2 = \frac{\Lambda \cap 2P}{2\Lambda}$. Let Λ_2 be the set

$$\{[x] \in \Lambda/2\Lambda : \forall [y] \in \Lambda/2\Lambda, x.y \equiv 0 \pmod{2} \text{ and } x^2 \equiv 0 \pmod{8}\}.$$

Notice that Λ_2 contains $\ker \iota_2$ and it can be explicitly computed as it only depends on Λ , which we know. Then one can see that Λ_2 contains two non-zero elements, say v_1, v_2 . As we assumed $[P : \Lambda] = 2$, only one between v_1 and v_2 is in $\ker \iota_2$.

As P is defined over $\mathbb{Q}(\sqrt{5})$, the Galois group

$$G := \text{Gal}(\mathbb{Q}(\sqrt{5})/\mathbb{Q}) = \langle \sigma \rangle \cong \mathbb{Z}/2\mathbb{Z}$$

acts on P and the kernel $\ker \iota_2$ is invariant under this action. By explicit computations, one can show that v_1 and v_2 are conjugated under the action of G , hence if one is in $\ker \iota_2$ also the other is, getting a contradiction.

We can then conclude that $[P : \Lambda] = 1$, that is, $\Lambda = \text{Pic } \bar{S}$. \square

Corollary 3.9. *The surface S is not birationally equivalent to the surface B arising from the Bhabha scattering in [35].*

Proof. Two K3 surfaces are birationally equivalent if and only if they are isomorphic. Two isomorphic K3 surfaces have isometric Picard lattices, which is not true for S and B , as $\text{rk Pic } \bar{B} = 20 \neq 19 = \text{rk Pic } \bar{S}$. This concludes the proof. \square

3.3 An application: computation of the Brauer group

In this subsection, we obtain information about the algebraic part of the Brauer group of $S = S_{DY}$ using the Galois module structure of $\text{Pic } \bar{S}$. Let $\text{Br } S$ denote the Brauer group of S and recall the filtration

$$\text{Br}_0 S \subseteq \text{Br}_1 S \subseteq \text{Br } S,$$

where $\text{Br}_0 := \text{im}(\text{Br}(\mathbb{Q}) \rightarrow \text{Br}(S))$ and $\text{Br}_1 := \ker(\text{Br } X_{DY} \rightarrow (\text{Br } \bar{S})^G)$, the algebraic part of $\text{Br } S$.

Earlier in Section 3 we have explicitly given a set of divisors Σ generating the whole geometric Picard lattice of X_{DY} . In particular it turns out that $\text{Pic } \bar{S}$ is defined over the field $\mathbb{Q}(\sqrt{5})$, quadratic extension of \mathbb{Q} . It follows that there is an action of the Galois group $G := \text{Gal}(\mathbb{Q}(\sqrt{5})/\mathbb{Q}) \cong \mathbb{Z}/2\mathbb{Z}$ over $\text{Pic } \bar{S}$. As Σ is invariant under the action of G , it becomes straightforward to explicitly describe the action using 19×19 matrices. Using this description it is then possible to compute the cohomology groups $H^i(G, \text{Pic } \bar{S})$ for every i .

Proposition 3.10. *The following isomorphisms hold:*

1. $H^0(G, \text{Pic } \bar{S}) \cong \mathbb{Z}^{18}$;
2. $H^1(G, \text{Pic } \bar{S}) \cong 0$;
3. $H^2(G, \text{Pic } \bar{S}) \cong (\mathbb{Z}/2\mathbb{Z})^{17}$.

Proof. Explicit Magma computations, see the attached Magma file [10]. \square

Corollary 3.11. *The quotient $\text{Br}_1 S / \text{Br}_0 S$ is trivial.*

Proof. As S is defined over \mathbb{Q} , a global field, from the Hochschild–Serre spectral sequence we have an isomorphism

$$\text{Br}_1 S / \text{Br}_0 S \cong H^1(G, \text{Pic } \bar{S})$$

(see, for example, [63, Corollary 6.7.8 and Remark 6.7.10]). From Proposition 3.10 it follows that $H^1(G, \text{Pic } \bar{S}) = 0$, proving the statement. \square

4 Elliptic fibrations on the surface

In this section, we explicitly describe some elliptic fibrations of the surface S which is used in Section 6 to re-obtain the full geometric Picard lattice of S in a different way.

After briefly recalling some basic notions concerning elliptic fibrations in Subsection 4.1, we present a general method to find elliptic fibrations on K3 surfaces with many -2 -curves (i.e., curves whose self-intersection is -2) in Subsection 4.2. We apply this method to the surface S , deriving some statistics about elliptic fibrations on S . In the last three subsections, we give the explicit description of three elliptic fibrations of S . The second fibration given in Subsection 4.4 is the one used in Section 6; the third fibration, given in Subsection 4.5 is the one used to give an explicit description of the Shioda–Inose structure of S (see Section 5). The first fibration is the simplest to compute and is the one that we originally used for the computations in Section 6. We include it here as another useful example although the second fibration is more straightforward to use for our purposes.

4.1 Background on elliptic fibrations

The *elliptic fibrations* of S are of interest for several reasons. In theoretical high energy particle physics, they play a crucial role since they can be used to analytically solve Feynman integrals in terms of elliptic multiple polylogarithms [20, 21, 73]. For this reason, a firm understanding of the elliptic fibrations of a given K3 surface can be critical in a particle physics computation. Apart from their important role in physics, they can also be used to provide an alternative proof of the full structure of $\text{Pic } \bar{S}$, as will be demonstrated in Section 6, and to compute other important arithmetic structures (Section 5).

Definition 4.1. An *elliptic fibration* is a morphism ϕ of S onto the projective line \mathbb{P}^1 (over $\bar{\mathbb{Q}}$) with general fibre a non-singular genus 1 curve, which has a section. A section of ϕ is a curve in S which maps isomorphically down to \mathbb{P}^1 under ϕ .

Equivalently, a section of ϕ is an irreducible curve in S whose intersection number with a fibre of ϕ (all of which are rationally equivalent) is 1. Two fibrations ϕ and ϕ_1 are said to be equivalent if there is an algebraic automorphism of \mathbb{P}^1 , α , such that $\phi_1 = \alpha \circ \phi$. Any such α is given by the standard $x \mapsto (ax+b)/(cx+d)$ action of an invertible 2-by-2 matrix $\begin{pmatrix} a & b \\ c & d \end{pmatrix}$ which is determined by α up to multiplication by a non-zero scalar. If only the morphism ϕ is given, without any section (and possibly having no section), then we call ϕ a *genus 1 fibration*.

Theorem 4.2 ([65]). *Let Y be a K3 surface. Then, genus-1 fibrations of Y (up to equivalence) are in 1-1 correspondence with divisor classes E in $\text{Pic } \bar{S}$ which satisfy*

1. $E.E = 0$ (E has self-intersection 0),
2. E is primitive (i.e., the class E is not divisible by any $n \geq 2$ in $\text{Pic } \bar{S}$),
3. E lies in the nef cone (i.e., E has non-negative intersection number with all classes in $\text{Pic } \bar{S}$ that represent effective divisors).

Under this correspondence, a genus-1 fibration ϕ is associated with the class of its fibres; conversely, a divisor class E satisfying the conditions 1,2,3 corresponds to the fibration map class given by the divisor map associated with the Riemann–Roch space of its global sections.

Proof. This is [65, Theorem 1] (cf [62, pp. 2–3]. For general results relating maps to projective space, invertible sheaves and divisor classes up to rational equivalence, see [42], Ch. 2, Sec. 7, and for specific results about general linear systems of K3 surfaces, see [67]. \square

If ϕ is a genus-1 fibration, the condition for the existence of a section is that there is another class D such that the intersection number $E.D$ is 1. By a slight transformation, it can then be seen that pairs of (fibration, section) correspond to 2-dimensional *hyperbolic* direct summands of the $\text{Pic } \overline{S}$ lattice. For a fixed fibration, any two distinct sections are mapped to each other under an isomorphism of S that preserves the fibration, viz. a translation map on the generic fibre extended to an automorphism of S . Since, ultimately, we are only interested in elliptic fibrations up to $\text{Aut } \overline{S}$, we will not worry too much about differentiating between different sections of an elliptic fibration. Our method for explicitly constructing fibrations gives genus-1 fibrations, although it also finds explicit sections in the majority of cases.

Definition 4.3. The *generic fibre* of a fibration $\phi : S \rightarrow \mathbb{P}^1$ over a field k , is the genus-1 curve $S_t/k(t)$ defined as the pullback of ϕ under the generic point inclusion $\text{Spec}(k(t)) \hookrightarrow \mathbb{P}^1$.

If s is a section of ϕ , then the analogous pullback gives a point $s_t \in S_t(k(t))$ which we can take as the O -point for an elliptic curve structure on S_t . When we talk about a fibration with a section, it is to be assumed that we are considering S_t as an elliptic curve with s_t as O . The surface S can be recovered from the generic fibre S_t , being isomorphic to the *Minimal (Curve) Model* over \mathbb{P}^1 of $S_t/k(t)$, which is characterised as a non-singular flat, proper scheme over (the Dedekind scheme) \mathbb{P}^1 , whose generic fibre is isomorphic to $S_t/k(t)$ and which has no -1 -curve as a component of any fibre. For more information on minimal models of curves, see [29, Chapter XIII].

As we shall see shortly, S has infinitely many elliptic fibrations up to equivalence. For any K3 surface, however, there are only finitely many classes of elliptic fibrations up to the action of $\text{Aut } \overline{S}$. There are some cases, using lattice computations on the full $\text{Pic } \overline{S}$, where a complete set of classes have been calculated (e.g. [19] and [9]), but we have not attempted to carry out such a computation here. Instead, we have used a method, described in the next subsection, for computing elliptic fibrations, which is independent of the knowledge of the full Picard group, and produces a large number of inequivalent fibrations when applied to S and the set of -2 -curves from the last section. An interesting subset of these fibrations, which we have used for various computations, will be given explicitly in the following subsections.

4.2 General method and results for the Drell–Yan surface

Consider a collection of -2 -curves, $\{C_i\}_{i \in I}$, on a smooth projective surface. Let

$$D = \sum_{i \in I} m_i C_i$$

be an effective divisor supported on a subset of the $\{C_i\}$. We refer to D as a *Kodaira fibre* when the configuration of the curves occurring in D is that of one of Kodaira’s singular

fibres for an elliptic fibration and they occur in D with the correct multiplicities for that type of fibre (see, e.g., [5, Chapter V, Section 7]). For example, $C_1 + C_2 + C_3$ is a Kodaira fibre of type I_3 if C_i and C_j meet transversally in a single point, for $1 \leq i < j \leq 3$, and the three intersection points are distinct.

The terminology that we use to refer to the type of a Kodaira fibre is the Dynkin style (except for \tilde{A}_n , I_n , \tilde{D}_n and \tilde{E}_n . Types *II*, *III* and *IV* do not occur in this paper.

Lemma 4.4. (a) *A Kodaira fibre on a K3 surface is always a singular fibre for an elliptic fibration of the surface.*

(b) *Distinct Kodaira fibres D_1, \dots, D_n lead to the same elliptic fibration up to equivalence if and only if they are pairwise disjoint (i.e., non-intersecting), in which case they give different singular fibres of that fibration.*

Proof. (a) This is just [70, Lemma 1.1], following easily from Theorem 4.2.

(b) Consider the fibration determined by D_1 . Since the curves in the other D_i do not intersect D_1 , they cannot cover the base \mathbb{P}^1 of the fibration. Thus they lie in fibres distinct from D_1 . Each D_i is connected, so lies in a single fibre. By Lemma 1.2 *loc. cit.*, and the fact that D_i has an irreducible constituent of multiplicity 1 by the definition of a Kodaira fibre, each D_i is the entire fibre. The fibres are distinct because the D_i are pairwise disjoint. \square

Remark 4.5. Equivalent elliptic fibrations have the same set of fibres and are completely determined by any one of those fibres. The fibres are all rationally equivalent and are the effective divisors of a single linear system $|D|$. The fibration is the one corresponding to that linear system up to equivalence: ϕ is the “divisor map” of $|D|$.

The method. Let Y be a K3 surface on which many -2 -curves are known. The method consists in constructing elliptic fibrations by searching for Kodaira fibres supported on these curves. Additionally, we hope to find explicit sections for a fibration from amongst the same set of curves.

1. Let \mathcal{S} be the set of known -2 -curves on Y .
2. Compute the intersection matrix M of the curves in \mathcal{S} .
3. Find all the Kodaira fibres supported by curves in \mathcal{S} (purely combinatorial).
4. Compute the elliptic fibration for interesting Kodaira fibres D , i.e., compute the Riemann–Roch space for D .
5. For a Kodaira fibre D , find a section in \mathcal{S} of the elliptic fibration determined by D , i.e., find a -2 -curve C supported in \mathcal{S} such that $D.C = 1$.

Remark 4.6. For the computations on the surface S in this paper, the set \mathcal{S} is defined below. The matrix M has been computed using `Magma` functionality to determine the intersection numbers between the strict transforms of divisors on the singular surface model and the exceptional divisors and also the local intersection numbers between the strict transforms over the singular points. We automated Step 3 of this method with a `Magma` function that takes M as argument. Step 4 was achieved using a slightly adapted version of `Magma`’s standard Riemann–Roch functionality. The computations also made use of the `Magma` function to impose additional Riemann–Roch conditions at singular points on the

surface in order to handle the exceptional divisors correctly. See the `Magma` file attached [10].

We have the -2 -curves L_i , $1 \leq i \leq 7$, and C_1, C_2 along with the fourteen $E_{i,j}$ exceptional divisors from the last section. Also, we have the transforms of the L_i and C_j under the $w \mapsto -w$ automorphism of S . We denote these transforms by \tilde{L}_i and \tilde{C}_j . Finally, we consider one final curve C_3 and its transform \tilde{C}_3 , where C_3 was also found as in Section 3 and is the strict transform on S of

$$C'_3: x^2 + yz = 0, \quad xy^2 - y^2z - xz^2 - yz^2 - w = 0.$$

Then we define

$$\mathcal{S} := \{L_i, \tilde{L}_i : 1 \leq i \leq 7\} \cup \{C_i, \tilde{C}_i : 1 \leq i \leq 3\} \cup \{E_{i,j}\},$$

a set of thirty-four -2 -curves on \bar{S} . In summary, we found the following results for \mathcal{S} .

Theorem 4.7. *Let $\Gamma \subset \text{Aut } \bar{S}$ be the subgroup of automorphisms generated by $w \mapsto -w$ and $\sqrt{5} \mapsto -\sqrt{5}$. Then on \bar{S} there are*

- 105,856 Kodaira fibres supported on \mathcal{S} , leading to
- 104,600 different genus-1 fibrations, 86,416 having a section in \mathcal{S} ;
- 29,111 fibrations inequivalent up to action of Γ , of which 27,807 have a section and 24,270 have a section in \mathcal{S} .

There are Kodaira fibres of types I_n , $2 \leq n \leq 14$ and $n = 16$; \tilde{D}_n , $n \leq 4 \leq 10$ and $n \in \{12, 14, 16\}$; and $\tilde{E}_6, \tilde{E}_7, \tilde{E}_8$.

Proof. By explicit computations. See the `Magma` file attached [10]. □

Remark 4.8. The number of distinct bad fibres entirely supported on \mathcal{S} in the various cases ranges from 1 to 5. The four-fibre cases have I_{10}, I_2, I_2, I_2 or $I_8, \tilde{D}_5, I_2, I_2$ type \mathcal{S} -supported fibres and the single five-fibre case has I_6, I_6, I_6, I_2, I_2 type \mathcal{S} -supported fibres. We have not computed the full sets of bad fibres in every case or attempted to determine how many classes of fibrations the 104,600 give under the full action of $\text{Aut } \bar{S}$ (and $\text{Gal}(\bar{\mathbb{Q}}/\mathbb{Q})$). They surely are many fewer in number than 29,111.

The following lemma gives the \mathcal{S} -Kodaira fibre data for three particular fibrations to be used in the next section of the paper. Explicit forms are given in the next three subsections. We note now that the first two have infinite Mordell–Weil groups, so by a result of Nikulin (cf. [62, Theorem 9]), *there are infinitely many inequivalent elliptic fibrations!*

Lemma 4.9. (a) *There is an elliptic fibration of S over \mathbb{Q} with three bad fibres consisting entirely of curves in \mathcal{S} :*

- (i) *an I_6 fibre, $L_1 + E_{2,1} + E_{2,-1} + \tilde{L}_1 + E_{5,-1} + E_{5,1}$;*
- (ii) *an I_6 fibre, $\tilde{L}_7 + L_7 + E_{4,2} + E_{4,1} + E_{4,-1} + E_{4,-2}$;*
- (iii) *a \tilde{D}_4 (I_0^*) fibre, $L_2 + \tilde{L}_2 + E_{3,-1} + E_{3,1} + 2E_{3,0}$;*

where the sums for the I_6 fibres give the components in cyclic order.

The L_i and \tilde{L}_i not occurring in one of these fibres along with the C_i , \tilde{C}_i and $E_{5,-2}$, $E_{5,2}$ all give sections of the fibration.

(b) There is an elliptic fibration of S over \mathbb{Q} with four bad fibres consisting entirely of curves in \mathcal{S} :

- (i) an I_{10} fibre, $L_6 + L_1 + E_{5,1} + E_{5,-1} + \tilde{L}_1 + \tilde{L}_6 + E_{4,2} + E_{4,1} + E_{4,-1} + E_{4,-2}$;
- (ii) an I_2 fibre, $C_1 + \tilde{C}_1$;
- (iii) an I_2 fibre, $C_2 + \tilde{C}_2$;
- (iv) an I_2 fibre, $C_3 + \tilde{C}_3$;

where the sum for the I_{10} fibre give the components in cyclic order.

The curves L_5 , \tilde{L}_5 , L_7 , \tilde{L}_7 , $E_{2,1}$, $E_{2,-1}$, $E_{3,1}$, $E_{3,-1}$, $E_{5,2}$, $E_{5,-2}$ all give sections of the fibration. All other curves in \mathcal{S} apart from these and the ones occurring in the above fibres give 2-sections or lie in other bad fibres.

(c) There is a genus-1 fibration of S over $\mathbb{Q}(\sqrt{5})$ with two bad fibres consisting entirely of curves in \mathcal{S} :

- (i) a \tilde{D}_8 (II^*) fibre, $6E_{4,-2} + 5E_{4,-1} + 4E_{4,1} + 4L_6 + 3\tilde{L}_3 + 3L_5 + 2E_{1,1} + 2E_{2,1} + E_{2,-1}$;
- (ii) another \tilde{D}_8 (II^*) fibre, $6\tilde{L}_2 + 5E_{5,-2} + 4E_{5,-1} + 4E_{3,0} + 3L_4 + 3E_{5,1} + 2E_{3,-1} + 2E_{5,2} + L_7$.

The fibration has no sections. However, there are a number of 2-sections provided by curves in \mathcal{S} : in particular, \tilde{L}_6 .

Proof. This follows from the Magma computations described above. The fact that the fibration in (c) has no section comes from the intersection matrix M , which shows that the intersection number of each curve in \mathcal{S} with either fibre is even. Note that \mathcal{S} generates $\text{Pic } \bar{S}$ (cf. Theorem 3.8). \square

4.3 First elliptic fibration

Proposition 4.10. (a) The generic fibre $S_t/\mathbb{Q}(t)$ of the elliptic fibration of Lemma 4.9 (a) has a Weierstrass equation

$$E_1 : y^2 = x^3 + (t-1)^2(t^2 + 6t + 1)x^2 - 16t^3(t-1)^2x.$$

(b) The full set of bad fibres for this fibration is given by the following fibres.

- The I_6, I_6, I_0^* fibres (i), (ii) and (iii) of Lemma 4.9. They lie over $t = \infty, 0, 1$, respectively.
- An I_2 fibre over $t = -1$ with components $E_{1,1}$ and the strict transform on S of the pullback on X of the plane curve $x + z = 0$.
- Four I_1 fibres over the points satisfying $t^4 + 8t^3 - 2t^2 + 8t + 1 = 0$.

(c) The group of points on $E_1(\mathbb{Q}(\sqrt{5})(t))$ generated by the \mathcal{S} -sections listed in Lemma 4.9 is isomorphic to

$$\mathbb{Z}/2\mathbb{Z} \oplus \mathbb{Z} \oplus \mathbb{Z},$$

where the first summand is generated by the 2-torsion point $(0, 0)$ and the two free ones are generated by the points

$$P_1 = (4t(t-1), -4t(t+1)(t-1)^2) \quad \text{and} \quad P_2 = (4t^3(t-1), -4\sqrt{5}t^3(t+1)(t-1)^2).$$

Proof. (a) Computing the Riemann–Roch space for Kodaira fibre (i) of Lemma 4.9 (a), using `Magma`, gives the fibration map

$$S \longrightarrow \mathbb{P}^1 \quad [x : y : z : w] \mapsto [z : x].$$

Letting $t = z/x$, we computed a singular plane model of S_t via elimination of w . We also computed the $\mathbb{Q}(t)$ -rational (non-singular) point corresponding to the L_5 section on this model of S_t . Then a curve Riemann–Roch computation using `Magma`'s function field machinery gives a Weierstrass model for S_t , which is easily simplified to the E_1 model given. The explicit isomorphism ψ from the plane model to E_1 is messy, and we do not write it down here.

(b) This follows easily from applying Tate's algorithm to the E_1 model.

(c) The points in $E_1(\mathbb{Q}(\sqrt{5})(t))$ corresponding to the sections were computed firstly on the plane model of S_t by the same specialisation and elimination of w , and then on E_1 using ψ . The result is then an easy lattice computation given the canonical height pairings between the points, which were computed for simplicity with the standard `Magma` intrinsic `HeightPairingMatrix`. Note that we could have also just used the intersection pairings from the matrix M , from which canonical heights are easily deduced since S is the minimal model of S_t . More computational details are in the attached `Magma` file [10] \square

Remark 4.11. There is a $t \mapsto 1/t$ symmetry and setting $s = t + (1/t) - 2$, we see that E_1 is the pullback under $\mathbb{Q}(s) \hookrightarrow \mathbb{Q}(t)$ of $Y^2 = X^3 + s(s+8)X^2 - 16sX$.

4.4 Second elliptic fibration

Proposition 4.12. (a) *The generic fibre $S_t/\mathbb{Q}(t)$ of the elliptic fibration of Lemma 4.9 (b) has a Weierstrass equation*

$$E_2 : y^2 = x^3 - (3t^4 + 8t^3 - 2t^2 - 1)x^2 + 16t^5(t^2 + t - 1)x.$$

(b) *The full set of bad fibres for this fibration is given by the following fibres.*

- *The I_{10}, I_2, I_2, I_2 fibres (i), (ii), (iii) and (iv) of Lemma 4.9. They lie over $t = 0, -(\sqrt{5} + 1)/2, (\sqrt{5} - 1)/2, \infty$, respectively.*
- *An I_4 fibre over $t = 1$ with components $L_2, \tilde{L}_2, E_{3,0}$ and the strict transform on S of the pullback on X of the plane curve $x - y = 0$.*
- *An I_2 fibre over $t = -1$.*
- *Two I_1 fibres over the points satisfying $t^2 + (2/9)t + (1/9) = 0$.*

(c) The group of points on $E_2(\mathbb{Q}(\sqrt{5})(t))$ generated by the \mathcal{S} -sections listed in the lemma is isomorphic to

$$\mathbb{Z}/2\mathbb{Z} \oplus \mathbb{Z},$$

where the first summand is generated by the 2-torsion point $(0, 0)$ and the free one is generated by the point

$$P_3 = (4t^3, 4t^3(t^2 - 1)).$$

Proof. Entirely analogous to the proof of Proposition 4.10. Here we find the elliptic fibration map

$$S \longrightarrow \mathbb{P}^1 \quad [x : y : x : w] \mapsto [x(y + z) : x^2 + yz]$$

and use the \mathbb{P}^1 parameter $t = x(y + z)/(x^2 + yz)$ and the $E_{2,-1}$ section to give a $\mathbb{Q}(t)$ -point on S_t . Again, see the attached Magma file [10] for computational details and explicit transformation maps. \square

4.5 Third elliptic fibration

The third example of Lemma 4.9 is a genus-1 fibration with no section. As shown in Section 5, however, this fibration provides a Shioda–Inose-type structure that furnishes much useful arithmetic and geometric information about S .

Proposition 4.13. (a) The generic fibre $S_t/\mathbb{Q}(\sqrt{5})(t)$ of the genus-1 fibration of Lemma 4.9 (c) is given by the quartic equation

$$\begin{aligned} ty^2 = & x^4 + ((-116\sqrt{5} + 272)t^2 + (66\sqrt{5} - 148)t - 34\sqrt{5} + 76)x^3 + \\ & ((-23664\sqrt{5} + 52974)t^4 + (62037\sqrt{5} - 138785)/2t^3 + (-71882\sqrt{5} + 160725)/2t^2 + \\ & (39297\sqrt{5} - 87871)/2t + (-3876\sqrt{5} + 8667)/2)x^2 + ((-2096932\sqrt{5} + 4689008)t^6 + \\ & (8789895\sqrt{5} - 19655187)/2t^5 + (-14213809\sqrt{5} + 31783015)/2t^4 + \\ & (14281062\sqrt{5} - 31933423)/2t^3 + (-10526810\sqrt{5} + 23538663)/2t^2 + \\ & (5316367\sqrt{5} - 11887758)/2t + (-98209\sqrt{5} + 219602)/2)x + \\ & ((-69643152\sqrt{5} + 155726921)t^8 + (191265401\sqrt{5} - 427682729)t^7 + \\ & (-1317057443\sqrt{5} + 2945029977)/4t^6 + (2349501743\sqrt{5} - 5253645563)/8t^5 + \\ & (-1901993416\sqrt{5} + 4252986577)/16t^4 + (19147095\sqrt{5} - 42814206)/4t^3 + \\ & (-250668666\sqrt{5} + 560512177)/8t^2 + (610197963\sqrt{5} - 1364444125)/8t + \\ & (-7465176\sqrt{5} + 16692641)/16). \end{aligned}$$

(b) The full set of bad fibres for this fibration is given by the following fibres.

- The II^* fibres (i) and (ii) of Lemma 4.9. They lie over $t = \infty, 0$, respectively.
- Four I_1 fibres over the points satisfying $t^4 - (1118\sqrt{5} + 2598)/27t^3 - (89700\sqrt{5} + 200362)/27t^2 - (1118\sqrt{5} + 2598)/27t + 1 = 0$.

Proof. (a) The Riemann–Roch computation for Kodaira fibre (i) in Lemma 4.9 is much longer and harder in this case than in the previous two, but it returned a fibration map $S \rightarrow \mathbb{P}^1$, $(x : y : z : w) \mapsto (b_1 : b_2)$, where b_1 and b_2 are two degree 9 weighted polynomials in x, y, z, w which we do not write down here, but are in Magma file [10].

As usual, letting $t = b_1/b_2$, we then computed a model for the generic fibre S_t of the fibration as a degree 10 plane curve C over $\mathbb{Q}(\sqrt{5})(t)$. Using the degree 2 divisor D on C provided by \tilde{L}_6 , and performing another Riemann–Roch Magma computation for D on a non-singular embedding of C in \mathbb{P}^9 , we explicitly determined the 2-to-1 cover $S_t \rightarrow \mathbb{P}^1$ corresponding to D . Finally, a standard computation using differentials gave us the equation for S_t in the statement. This is laid out in Magma file [10].

(b) By the choice of b_1, b_2 , the bad fibres over 0 and ∞ are the two II^* fibres. To compute the other bad fibres, a $t = s^2$ substitution (giving a base change unramified over $0, \infty$) allows the transformation to a Weierstrass cubic model and standard application of Tate’s algorithm. This shows that the only other bad fibres of S_t are I_1 fibres at the stated points. \square

Remark 4.14. Shioda–Inose structures associated with this fibration are made explicit in Section 5. We briefly include some extra information on that topic here.

There is a *Nikulin involution*, ι ([57], Sec. 5), which is an algebraic involution of S over $\mathbb{Q}(\sqrt{5})$ which swaps the 2 II^* fibres and for which the desingularised quotient $Y = S/\langle \iota \rangle$ is a Kummer surface.

From the explicit quartic equation above, it is not too hard to show that ι is the involution of S associated with the isomorphism ι^* of the function field $k(S) = k(t, x, y)$ ($k = \mathbb{Q}(\sqrt{5})$)

$$\begin{aligned} \iota^* : k(t, x, y) &\cong k(t, x, y) \\ t &\mapsto 1/t \quad x \mapsto \alpha x + \beta \quad y \mapsto -\gamma y \end{aligned}$$

where

$$\alpha = t^{-2} \left(\frac{t+e}{et+1} \right) \quad \beta = ((3035 - 1302\sqrt{5})/38) \left(\frac{(t-1)(t^2+ft+1)}{t^2(et+1)} \right) \quad \gamma = t\alpha^2$$

with

$$e = (138 + 67\sqrt{5})/19 \quad f = (2770 + 1324\sqrt{5})/355.$$

The following diagram commutes

$$\begin{array}{ccc} S & \xrightarrow{\iota} & S \\ \downarrow & & \downarrow \\ \mathbb{P}^1 & \xrightarrow{t \mapsto 1/t} & \mathbb{P}^1 \end{array}$$

and Y has a genus-1 fibration with generic fibre over $k(s)$, $s = t + (1/t) - 2$, with quartic equation $sy_1^2 = F(x_1)$ for a degree 4 monic polynomial F over $k(s)$. Here $x_1 = x + \iota^*(x)$ and y_1 is an element of $k(s)$ times $y + \iota^*(y)$. We do not write down the polynomial F but it comes from the explicit computation of $k(s, x_1, y_1) = k(t, x, y)^{\langle \iota^* \rangle}$. This computation and the explicit F are in Magma file [10]. Y is the minimal model over \mathbb{P}^1 of this genus 1 curve.

5 Computation of the Shioda–Inose structure

In this section, we exhibit an explicit Shioda–Inose structure of the surface S_{DY} ; in doing so, we closely follow the exposition in [57] and [60].

Let X be any smooth algebraic surface over \mathbb{C} . The singular cohomology group $H^2(X, \mathbb{C})$ admits a Hodge decomposition

$$H^2(X, \mathbb{C}) \cong H^{2,0}(X) \oplus H^{1,1}(X) \oplus H^{0,2}(X).$$

The Néron–Severi group $\text{NS}(X)$ of line bundles modulo algebraic equivalences naturally embeds into $H^2(X, \mathbb{Z})$ and can be identified with $H^2(X, \mathbb{Z}) \cap H^{1,1}(X)$. This induces a structure of a lattice on $\text{NS}(X)$. Its orthogonal complement in $H^2(X, \mathbb{Z})$ is denoted by T_X and is called the *transcendental lattice* of X .

If X is a K3 surface the lattice $H^2(X, \mathbb{Z})$ is isometric to the lattice $U^3 \oplus E_8(-1)^2$ where $E_8(-1)$ denotes the standard E_8 -lattice with opposite pairing, corresponding to the Dynkin diagram E_8 . The lattice U is the hyperbolic lattice which is generated by vectors x, y such that $x^2 = y^2 = 0$ and $x \cdot y = 1$. Moreover, $\dim H^{2,0}(X) = 1$. Any involution ι on X such that $\iota^*(\omega) = \omega$ for a non-zero $\omega \in H^{2,0}(X)$ is called a *Nikulin involution*.

Remark 5.1. Recall that for a K3 surface the notions of Picard group and Néron–Severi group coincide (cf. [48, Proposition 1.2.4]).

It follows from [61, Section 5] (see also [57, Lemma 5.2]) that every such involution has eight isolated fixed points and the rational quotient $\pi : X \dashrightarrow Y$ by a Nikulin involution gives a new K3 surface Y .

Definition 5.2 ([57, Definition 6.1]). A K3 surface X admits a Shioda–Inose structure if there is a Nikulin involution on X and the quotient map $\pi : X \dashrightarrow Y$ is such that Y is a Kummer surface and π_* induces a Hodge isometry $T_X(2) \cong T_Y$.

Every Kummer surface admits a degree 2 map from an abelian surface A . It follows from [57, Theorem 6.3] that if X admits a Shioda–Inose structure (Figure 1) then $T_A \cong T_X$.

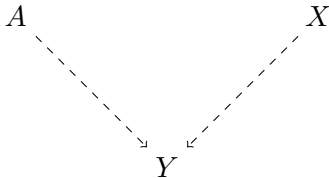


Figure 1. Shioda–Inose structure.

This follows from the fact that the diagram induces isometries $T_A(2) \cong T_Y$ and $T_X(2) \cong T_Y$. Alternatively, this is equivalent to the existence of an embedding $E_8(-1)^2 \hookrightarrow \text{NS}(X)$.

5.1 Shioda–Inose structure on the Drell–Yan K3 surface

Let S be the model of the Drell–Yan K3 surface introduced in Section 4 in Proposition 4.13. The pullback of the generic fibre S_t by the map $t \mapsto t^2$ produces a Kummer surface \mathcal{K} with

an explicit elliptic fibration \mathcal{I} . The fiber \mathcal{I}_t above the point t has equation

$$y^2 = x^3 + \frac{1}{6} \left(-45\sqrt{5} - 71 \right) t^4 x + \frac{1}{2} \left(3 - \sqrt{5} \right) t^8 + \frac{1}{27} \left(-189\sqrt{5} - 551 \right) t^6 + \frac{1}{2} \left(3 - \sqrt{5} \right) t^4.$$

Let $E_{a,b}$ and $E_{c,d}$ be the two elliptic curves defined by

$$\begin{aligned} E_{a,b}: y^2 &= x^3 + ax + b, \\ E_{c,d}: y^2 &= x'^3 + cx' + d. \end{aligned}$$

Consider the abelian surface $E_{a,b} \times E_{c,d}$ given by the product of the two elliptic curves defined above, and let $[-1]$ denote the automorphism of $E_{a,b} \times E_{c,d}$ given by multiplication by -1 . Taking the quotient of $E_{a,b} \times E_{c,d}$ by $[-1]$, we obtain a Kummer surface which has a natural elliptic fibration with parameter u :

$$x^3 + ax + b - u^2(x'^3 + cx' + d) = 0.$$

This can be converted into the following Weierstrass model, cf. [52, §2.1]

$$Y^2 = X^3 - 3acX + \frac{1}{64}(\Delta_{E_{a,b}}u^2 + 864bd + \frac{\Delta_{E_{c,d}}}{u^2}). \quad (5.1)$$

The elliptic fibration \mathcal{I} is isomorphic to (5.1). Hence, up to scaling, we obtain the following system of equations:

$$\begin{aligned} A^2 - 5 &= 0, \\ 1411985089 - 631459755A + 18ac &= 0, \\ 131587540863282 - 58847737271814A + 108c^3 + 729d^2 &= 0, \\ -238992218766044 + 106880569389324A - 1458bd &= 0, \\ 131587540863282 + 108a^3 - 58847737271814A + 729b^2 &= 0. \end{aligned}$$

Let \mathcal{P} be the scheme defined by the above system of equations. Let K denote the number field

$$K = \mathbb{Q} \left(\sqrt{2}, \sqrt{5}, \alpha = \sqrt{\frac{\sqrt{5}+1}{2}}, \beta = \sqrt[3]{\sqrt{2}-1} \right).$$

Remark 5.3. The field K is isomorphic to $\mathbb{Q}[x]/(x^{24} - 24x^{18} - 18x^{12} + 24x^6 + 1)$.

The scheme \mathcal{P} has four K -rational points. As each K -rational point of \mathcal{P} (i.e., a solution of the system over K) provides an isomorphic Shioda–Inose structure, we consider the one given by the following coordinates:

$$\begin{aligned} A &= \sqrt{5}, \\ a &= \frac{1}{6} \left(10611\sqrt{2} - 18087\sqrt{5} - 4775\sqrt{10} + 40515 \right) \beta, \\ b &= \frac{1}{27} \left(-4779461\sqrt{5} + 26\sqrt{2} \left(113888 - 50921\sqrt{5} \right) + 10686297 \right) \alpha, \\ c &= \frac{1}{6} \left(16 \left(832\sqrt{5} - 1869 \right) \sqrt{2} + 8537\sqrt{5} - 19293 \right) \beta^2, \\ d &= \frac{1}{27} \left(26 \left(50921\sqrt{5} - 113888 \right) \sqrt{2} - 4779461\sqrt{5} + 10686297 \right) \alpha. \end{aligned}$$

Let $E_{\mu,\nu}$ denote the elliptic curve given by

$$y^2 = x^3 + 4x^2 + 2(1 - 4\mu\sqrt{2} - 3\nu\sqrt{5})x,$$

with $\mu, \nu = \pm 1$. The elliptic curve $E_{a,b}$ is isomorphic to $E_1 = E_{1,1}$ and $E_{c,d}$ is isomorphic to $E_2 = E_{-1,1}^{(-1)}$; both isomorphisms are *a priori* only defined over $\overline{\mathbb{Q}}$.

Proposition 5.4. *The Kummer surface $\mathcal{K} = \text{Kum}(E_1, E_2)$ attached to the abelian variety $E_1 \times E_2$ is isomorphic to the elliptic surface \mathcal{I} over the field $\mathbb{Q}(\sqrt{2}, \sqrt{5}, \eta)$, where $\eta = -\sqrt{74\sqrt{5} - 2\sqrt{4329\sqrt{5} + 10267} + 117}$.*

Proof. The natural elliptic fibration on \mathcal{K} is provided by the genus 1 curve

$$\mathcal{K}_t : x^3 + 4x^2 + 2(1 - 4\sqrt{2} - 3\sqrt{5})x - t^2(y^3 - 4y^2 + 2(1 + 4\sqrt{2} - 3\sqrt{5})y) = 0.$$

It follows from a direct computation that the equation $\mathcal{K}_{t/\eta}$ is isomorphic to \mathcal{I}_t via the automorphism $(x, y) \mapsto (xu^2, yu^3)$ where $u = (\eta/2)^2$. \square

Let $E_{256.1-i2}$ denote the elliptic curve with the LMFDB label 4.4.1600.1-256.1-i2. Its Weierstrass equation is

$$E_{256.1-i2} : y^2 = x^3 + 2(\sqrt{2} + 1)x^2 + \frac{1}{2}(-10\sqrt{2} + 9\sqrt{5} + 6\sqrt{10} - 13)x.$$

The curve $E_{256.1-i2}$ is the quadratic twist of $E_{1,1}$ by the element $\frac{1}{2} + \frac{1}{\sqrt{2}}$.

Proposition 5.5. *Let ρ denote the unique 2-dimensional Artin representation of the field $\mathbb{Q}[x]/(-4 + 4x^2 + x^4)$. For each prime $p \neq 2, 5$ we have the equality*

$$L_p(E_{256.1-i2} \otimes \rho, s) = L_p(E_{1,1}, s)^2,$$

where L_p denotes the p -th Euler factor.

Proof. The conclusion follows from the fact that both elliptic curves are related by a quadratic twist. We then compute the representation ρ , which corresponds to this twist. \square

The elliptic curve E_1 is a \mathbb{Q} -curve which is modular. The corresponding automorphic form is a twist of the Hilbert modular \mathcal{H} form with label 4.4.1600.1 - 256.1 - i in the LMFDB notation. The form above is a base change. In particular, the Weil restriction $\text{Res}_{\mathbb{Q}}^K E_1$ is an abelian variety of dimension 4 which is isogenous to a product of two abelian surfaces A, B and we have

$$L(\text{Res}_{\mathbb{Q}}^K E_1, s) = L(A, s)L(B, s).$$

Remark 5.6 (Description of the isogeny class). Consider the map $\phi : E_1 \rightarrow E_2$ defined by

$$\phi(x, y) = (\phi_x(x), \phi_y(x, y)) \tag{5.2}$$

where

$$\begin{aligned}\phi_x(x) &:= \frac{x(7x^2 + 6(\sqrt{2} + 5)x - 2\sqrt{5}(x+3)(\sqrt{2}x+3) + 54)}{9x^2 - 6(3\sqrt{5} + \sqrt{2}(\sqrt{5} + 3) + 1)x + 18\sqrt{5} + 4\sqrt{2}(5\sqrt{5} + 9) + 74}, \\ \phi_y(x, y) &:= \frac{1}{D_y(x)} \left((63x + 142)x - \sqrt{5}(((11x + 23)x + 34)x + 72) + \right. \\ &\quad \left. + \sqrt{2}(((17x + 38)x + 82)x - 2\sqrt{5}((9x + 19)x + 12) + 72) + 192 \right) y, \\ D_y(x) &:= -27x^3 + 27(3\sqrt{5} + \sqrt{2}(\sqrt{5} + 3) + 1)x^2 + \\ &\quad - 18(9\sqrt{5} + 2\sqrt{2}(5\sqrt{5} + 9) + 37)x + \\ &\quad + 8(54\sqrt{5} + \sqrt{2}(32\sqrt{5} + 81) + 95).\end{aligned}$$

The map ϕ is an isogeny of degree 3; the kernel of ϕ is generated by a point with x -coordinate $1/3(\sqrt{5} + 3)\sqrt{2} + 1/3(3\sqrt{5} + 1)$.

Let $\psi : E_1 \rightarrow F$ be a unique 2-isogeny over K_4 from E_1 and $\psi' : E_2 \rightarrow G$ be the unique 2-isogeny over K_4 from E_2 .

Let $\mathcal{E}^{(d)}$ denote the quadratic twist by d of an elliptic curve \mathcal{E} . We have the following isomorphisms over K_4 .

$$\begin{aligned}E_{1,1} &= E_1 & E_{-1,1} &\cong E_2^{(-1)} \\ E_{1,-1} &\cong G^{(2)} & E_{-1,-1} &\cong F^{(-2)}\end{aligned}$$

There exists also a 7-isogeny from $E_{1,1}$ to the elliptic curve

$$\tilde{E} : y^2 = x^3 + 4(18\sqrt{10} + 49)x^2 + (-7888\sqrt{2} - 5046\sqrt{5} + 3528\sqrt{10} + 11282)x,$$

which is induced by the cyclic subgroup generated by the point with x -coordinate $(\sqrt{5} - 5)\sqrt{2} - 3\sqrt{5} + 3$. In total we have a cubic configuration of 2,3,7 isogenies, cf. Figure 2.

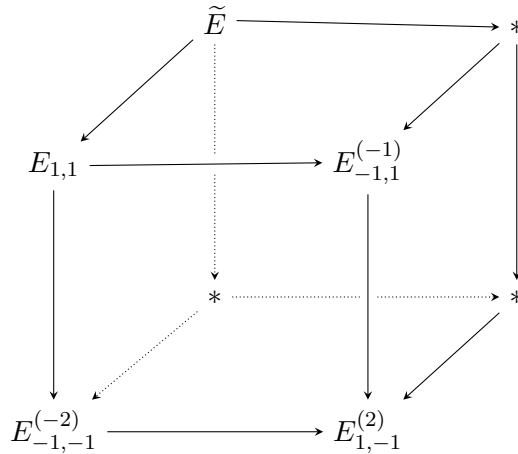


Figure 2. Left-to-right maps: degree 3; up-to-down maps: degree 2; back-to-front maps: degree 7. A star denotes an explicit elliptic curve which can be computed from the given isogeny.

Theorem 5.7. *Let E_1, E_2 be the two elliptic curves defined over the field $K_4 = \mathbb{Q}(\sqrt{2}, \sqrt{5})$ by the following equations:*

$$\begin{aligned} E_1 : y^2 &= x^3 + 4x^2 + 2(1 - 4\sqrt{2} - 3\sqrt{5})x, \\ E_2 : y^2 &= x^3 - 4x^2 + 2(1 + 4\sqrt{2} - 3\sqrt{5})x. \end{aligned}$$

They are 3-isogenous over K_4 . There is a Shioda–Inose structure on S with the Kummer surface $\text{Kum}(E_1 \times E_2)$. Let $p \geq 7$ be a prime number. We have that

$$|S(\mathbb{F}_p)| = 1 + 17p + \left(1 + \left(\frac{5}{p}\right)\right)p + H(p) + p^2$$

with $H(p)$ satisfying

$$H(p) = \begin{cases} a_{\mathfrak{p}}^2 - p, & \text{if } p \text{ splits completely in } K_4, \\ -\epsilon(p)p, & \text{if } p \text{ splits into two primes in } K_4 \text{ and } a_{\mathfrak{p}} = 0, \\ -a_{\mathfrak{p}} + \epsilon(p)p, & \text{otherwise,} \end{cases}$$

where $\epsilon(p) = \left(\frac{10}{p}\right)$ and $a_{\mathfrak{p}}$ is the eigenvalue at \mathfrak{p} (we take any prime ideal in the decomposition) of the Hilbert modular form \mathcal{H} .

Moreover, for $p \geq 7$ the number of points over \mathbb{F}_{p^2} satisfies the formula

$$|S(\mathbb{F}_{p^2})| = 1 + 18p^2 + t(p)^2 + p^4,$$

where $t(p)$ is the trace of the Frobenius on \mathbb{F}_{p^2} acting on the reduction of the curve E_1 .

Proof. It follows from Proposition 4.12 that there exists a basis of the Néron–Severi group of S in which all the elements of the basis are defined over \mathbb{Q} except for the components not intersecting the zero section of the singular fibres above $t = \frac{1}{2}(-1 \pm \sqrt{5})$. Under the action of an element $\sigma \in \text{Gal}(\overline{\mathbb{Q}}/\mathbb{Q})$ such that $\sigma(\sqrt{5}) = -\sqrt{5}$ the two components are permuted. Hence we conclude by Grothendieck–Lefschetz trace formula [42, Appendix C §4] that for a prime number p of good reduction for S we have

$$|S(\mathbb{F}_p)| = 1 + 17p + \left(1 + \left(\frac{5}{p}\right)\right)p + H(p) + p^2.$$

The number $H(p)$ corresponds to the trace of the Frobenius endomorphism Frob_p acting on the three-dimensional subspace H of $H_{\text{et}}^2(S_{\overline{\mathbb{F}}_p}, \mathbb{Q}_{\ell})$, $\ell \neq p$, which is the complement of the image of the Néron–Severi group via the cocycle map.

From the existence of the Shioda–Inose structure on S we know that the structure is parametrized by two elliptic curves $E_{a,b}$ and $E_{c,d}$. We find isomorphic (over $\overline{\mathbb{Q}}$) models of $E_{a,b}$ and $E_{c,d}$, respectively E_1 and E_2 . From Proposition 5.4 it follows that $\text{Gal}(\overline{\mathbb{F}}_p/\mathbb{F}_{p^4})$ the space H and $\text{Sym}^2 H_{\text{et}}^1((E_1)_{\overline{\mathbb{F}}_p}, \mathbb{Q}_{\ell})$ are isomorphic as Galois modules. This follows from the existence of the 3-isogeny between E_1 and E_2 .

The surface S is isomorphic to the Inose fibration over $K_8 = \mathbb{Q}(\sqrt{2}, \sqrt{5}, \eta) = \mathbb{Q}[x]/(x^8 - 4x^6 + 7x^4 - 6x^2 + 1)$ due to Proposition 5.4. The Galois group of the field K_8 is $C_2 \times D_4$. So, if the eigenvalues of the Frobenius Frob_{p^2} acting on $H_{\text{et}}^1((E_1)_{\overline{\mathbb{F}}_p}, \mathbb{Q}_{\ell})$ are α, β , then the

eigenvalues of Frob_{p^2} acting on $\text{Sym}^2 H_{\text{et}}^1((E_1)_{\overline{\mathbb{F}}_p}, \mathbb{Q}_\ell)$ are $\alpha^2, \beta^2, \alpha\beta$ and hence the trace of Frob_{p^2} on $\text{Sym}^2 H_{\text{et}}^1((E_1)_{\overline{\mathbb{F}}_p}, \mathbb{Q}_\ell)$ is the same as the trace of Frob_{p^2} on H . Hence, the formula for the number of points in $S(\mathbb{F}_{p^2})$ follows.

It follows from Propositions 5.4 and 5.5 that the trace $H(p)$ of Frob_p acting on H is computed by the following recipe.

1. The elliptic curve $E_{1,1}$ is modular and corresponds to a twist of the Hilbert modular form \mathcal{H} attached to $E_{256.1-i2}$.
2. The form \mathcal{H} is defined over $\mathbb{Q}(\sqrt{2}, \sqrt{5})$ and is of parallel weight $[2, 2, 2, 2]$.
The corresponding automorphic representation $\pi_{\mathcal{H}}$ has an L -function $L_{\mathcal{H}} = L(\pi_{\mathcal{H}}, s)$ of degree 4.
3. The symmetric square L -function $\text{Sym}^2 L_{\mathcal{H}}$ corresponds to the motive

$$\mathcal{M} = \text{Sym}^2 H^1(E_{256.1-i2})$$

attached to the elliptic curve $E_{256.1-i2}$.

4. Hence the trace of Frob_p on the ℓ -adic realisation of \mathcal{M} is given by the recipe $a_{\mathfrak{p}}^2 - p$ for a prime p which splits completely in $\mathbb{Q}(\sqrt{2}, \sqrt{5})$ and $a_{\mathfrak{p}} - p$ for a prime which does not split completely.
5. To conclude the theorem we have to twist by a character ψ of order 4 which satisfies the property $\psi(p)^2 = 1$ for a split prime p , $\psi(p) = -\epsilon(p)$ for a non-split prime with $a_{\mathfrak{p}} = 0$ and $\epsilon(p)$ otherwise.
6. Finally, the Hilbert modular form \mathcal{H} is twisted by ϵ , as well.

□

5.2 Supersingular reduction

The Drell–Yan K3 surface has Picard rank 19 in characteristic 0. When we reduce to characteristic p the Picard rank can jump to 20 (ordinary reduction) or 22 (supersingular reduction). We describe here under what conditions we have a supersingular reduction. Conjecturally, based on the Lang–Trotter prediction the set of supersingular primes has density zero among all primes. However, the result of Elkies [33] proves that there are infinitely many supersingular primes for the surface S .

Corollary 5.8. *For primes p such that $j \in \mathbb{F}_{p^2}$ is a supersingular j -invariant, we have that $\text{NS}(S_{\overline{\mathbb{F}}_p})$ is of rank 22, i.e., the prime p is of supersingular reduction. The set of primes of supersingular reduction is infinite.*

Proof. The rank $\rho(p)$ of the group $\text{NS}(S_{\overline{\mathbb{F}}_p})$ is equal to $18 + \text{rank Hom}(\tilde{E}_1, \tilde{E}_2)$ for a reduction modulo p of the curves E_1, E_2 . Since the curves E_1, E_2 are linked by an isogeny and they do not have complex multiplication, it follows that $\text{rank Hom}(\tilde{E}_1, \tilde{E}_2) = 1$ unless they have supersingular reduction at p . Since E_1, E_2 are defined over a field with at least one real embedding, it follows from [33] that there are infinitely many supersingular primes. □

Remark 5.9. It follows from the standard Lang–Trotter type prediction that the set of supersingular primes of E_1, E_2 is of density zero within the set of primes, cf. [33].

To compute the primes of supersingular reduction in practice, we perform the following algorithm. First, we compute the minimal polynomial of the j -invariant of the curve E_1 , namely

$$P(T) = T^4 - 6416768T^3 + 12470497280T^2 + 27021904707584T - 34447407894757376.$$

The elliptic curve E_1 has supersingular reduction at a prime ideal \mathfrak{p} above a rational prime p if the polynomial $P(T)$ modulo p has a common root with the polynomial $S_p(T) = \prod_j (T - j)$, where the product is over supersingular j -invariants. The latter is computed effectively, cf. [71, V], [36]. In fact, we checked all the odd primes p smaller than 104729 and the elliptic curve E_1 modulo p is supersingular for the following values of p :

13, 29, 41, 113, 337, 839, 853, 881, 953, 1511, 1709, 1889, 2351, 3037, 3389, 4871, 5557, 5711, 5741, 6719, 6733, 7237, 8821, 14489, 14869, 14951, 15161, 15791, 15973, 18229, 18257, 18313, 18341, 20021, 21517, 23197, 24359, 26921, 27749, 28559, 33349, 33461, 33599, 34649, 37813, 40151, 44101, 45389, 47629, 49057, 50077, 50231, 52919, 54277, 54377, 58631, 60689, 64679, 65269, 68879, 69761, 70237, 70309, 72269, 72911, 78791, 91309, 101501.

6 Computing the Picard lattice via elliptic fibrations

This is the section on the computation of $\text{Pic } \bar{S}$ based on elliptic fibrations on S . Recall that: S is the desingularisation of the surface $X_{DY} \subset \mathbb{P}^3$ defined in (1.1); the map $\pi: S \rightarrow \mathbb{P}^1$ is the elliptic fibration defined in Proposition 4.12; we denote by T the image in $\text{Pic } S$ of a torsion section of π (for example $(0, 0)$), by F the image of the general fiber E_2 , and by O the image of the zero section; finally we denote by $\text{NS}(\bar{S}) = N$ the geometric Néron–Severi group of S .

Remark 6.1. As already noted in Remark 5.1, on a K3 surface the notions of Picard group and Néron–Severi group coincide, hence $\text{Pic } \bar{S} = N$. In this section, we use the latter notion instead of the former, in contrast to the rest of the paper, as an homage to Shioda’s work, whose results, contained in [69], are the key ingredients of this section.

Every singular fibre $\pi^{-1}(v)$ of the fibration π has type I_n and we order the components in a cyclic order, cf. [69], i.e., θ_i^v for $i = 0, \dots, n - 1$, component θ_v^i intersects once the components θ_v^{i-1} and θ_v^{i+1} (enumeration modulo n). The component θ_v^0 is the unique component that intersects the zero fibre.

The Néron–Severi group of an elliptic surface is generated by the following divisors:

- all components of the singular fibres,
- the image of a general non-singular fibre,
- images of sections which correspond bijectively to points in the Mordell–Weil group of the generic fibre.

Since the numerical and algebraic equivalence coincide on an elliptic surface [69], it follows that it is enough for the Néron–Severi group to consider the spanning set which contains only the components of the reducible fibres which do not intersect the zero component.

Proposition 6.2. *The Néron–Severi group N of S is a lattice of rank 19 and discriminant 24. It is spanned by $P = P_3, T, F, O$, and the components of the singular fibres in fibration π which do not intersect the zero section O and lie above the following points:*

- $t = 0$: components $a_i = \theta_{t=0}^i$ for $i = 1, \dots, 9$;
- $t = -1$: component $\theta_{t=-1}^1$;
- $t = \frac{1}{2}(-1 \pm \sqrt{5})$: components θ_{\pm}^1 ;
- $t = 1$: components $b_i = \theta_{t=1}^i$, $i = 1, 2, 3$.

The dual graph of the -2 -curves which generate the Néron–Severi group is represented in Figure 3. We include for completeness also the component of the fibre above $t = \infty$ which is not used in the basis. Each edge $A - B$ represents a unique transversal intersection between curves A and B .

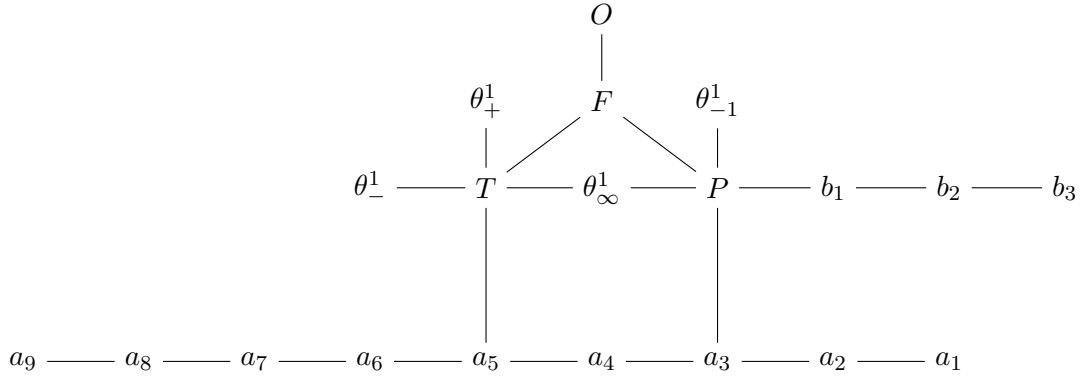


Figure 3. The dual graph of the -2 -curves which generate the Néron–Severi group.

6.1 A different proof

In this subsection we prove Proposition 6.2. For the convenience of the reader, we split the proof in four main steps, each corresponding to a subsubsection. The computation of the rank still relies on Proposition 3.5, but not on the divisors exhibited in Section 3; the computation of the discriminant only relies on the elliptic fibration presented in Subsection 4.4.

6.1.1 The rank

The Shioda–Tate formula [69] tell us that the rank of the group N is bounded from below by 19 and by Lefschetz theorem on $(1,1)$ -classes [47, Theorem 3.3.2] it is bounded by 20 from above. It follows from Proposition 3.5 that the upper bound on the rank is 19. Hence the group N has rank 19. To perform the computations from Proposition 3.5 one could apply a point count directly deduced from the Weierstrass equation of the given elliptic fibration, cf. [58, 59, 75].

6.1.2 Height pairing computations

Shioda [69, Theorem 8.6] defined the quadratic positive semi-definite height pairing $\langle \cdot, \cdot \rangle$ on the group $E_2(\overline{\mathbb{Q}}(t))$ which explicitly on the point P is

$$\langle P, P \rangle = 4 - \frac{a_0(10 - a_0)}{10} - \sum_{i=1}^4 \frac{a_i(2 - a_i)}{2} - \frac{a_5(4 - a_5)}{4}$$

for a suitable choice of correction values a_i , $a_0 \in \{0, \dots, 9\}$, $a_1, a_2, a_3, a_4 \in \{0, 1\}$, $a_5 \in \{0, 1, 2, 3, 4\}$, cf.[69, p. 22]. It follows from the Tate algorithm [74], [72, IV,§9] that for the point $P_3 = (4t^3, 4t^3(t^2 - 1))$ the height $\langle P_3, P_3 \rangle$ equals $3/20$. The minimal positive theoretically possible height of the point in $E_2(\overline{\mathbb{Q}}(t))$ is equal to $1/20$ which follows from the height formula described above. The free part of $E_2(\overline{\mathbb{Q}}(t))$ is of rank 1. Hence if $P_3 + \mathcal{T}$ were m -divisible for a suitable choice of a torsion point \mathcal{T} , then the height of the point Q such that $mQ = P_3 + \mathcal{T}$ would be equal to $\frac{3}{20m^2} < \frac{1}{20}$ for any $m \geq 2$, in contradiction to the minimality of height. Hence, the point P_3 spans the free part of $E_2(\overline{\mathbb{Q}}(t))$.

6.1.3 Discriminant formula

As E_2 is the generic fibre of the elliptic fibration $S \rightarrow \mathbb{P}^1$, the discriminant of N can be computed from the discriminant formula, cf.[68, §11.10]

$$\text{disc } N = (-1)^r \text{disc Triv} \cdot \text{disc MW}(S) / |\text{MW}(S)_{\text{tors}}|^2$$

where r is the rank of the group $E_2(\overline{\mathbb{Q}}(t))$, disc Triv is the discriminant of the trivial sublattice with respect to the natural intersection pairing on N , $\text{disc MW}(S)$ is the discriminant of the lattice $E_2(\overline{\mathbb{Q}}(t))/E_2(\overline{\mathbb{Q}}(t))_{\text{tors}}$ with respect to the height pairing $\langle \cdot, \cdot \rangle$ and $\text{MW}(S)_{\text{tors}}$ is $E_2(\overline{\mathbb{Q}}(t))_{\text{tors}}$. In our case we obtain $\text{disc } N = 96/T^2$ where the integer $T \geq 1$ is the order of the torsion subgroup in $E_2(\overline{\mathbb{Q}}(t))$. Since $\text{disc } N$ is an integer, it follows that $T|2^2$. We have a unique point of order 2 in $E_2(\overline{\mathbb{Q}}(t))$ since the cubic polynomial which defines E_2 has only one root in $\overline{\mathbb{Q}}(t)$. If there is a point P_4 of order 4 on this curve, then $2P_4 = (0, 0)$. For a general point (x, y) on E_2 the x -coordinate of the point $2(x, y)$ is

$$\frac{(16t^7 + 16t^6 - 16t^5 - x^2)^2}{4x(16t^7 + 16t^6 - 16t^5 - 3t^4x - 8t^3x + 2t^2x + x^2 + x)}.$$

Hence if $(0, 0)$ were 2-divisible, the polynomial $x^2 - 16t^5(t^2 + t - 1)$ would have a root over $\overline{\mathbb{Q}}(t)$, which is impossible.

Hence we conclude that the Néron–Severi group N is spanned by the components of the trivial sublattice (root sublattice generated by components of the fibres and the image of the zero section) and by the curve in N representing P_3 and the torsion section $(0, 0)$. Its discriminant is equal to 24. We have also shown that

$$E_2(\overline{\mathbb{Q}}(t)) = E_2(\mathbb{Q}(\sqrt{5})(t)).$$

6.1.4 Néron–Severi group basis

The group N is spanned by the components of the reducible fibres, the general fibre F , the image of the zero section O and the images of the non-zero sections which generate the Mordell–Weil group of the generic fibre. In our case, we have two points P and T , where P is of infinite order, and T is a generator of the torsion subgroup (2-torsion point). We consider a generating set \mathcal{B} for N , which contains only the following curves:

- the components θ_v^i for $i > 0$ of the reducible fibres (we skip the component which meets the zero section),
- the zero section O ,
- the general fibre F ,
- the sections P and T .

The intersection pairing matrix for the tuple of curves above has dimension 20 and rank 19. The curves satisfy the following linear relation:

$$a_1 + 2a_2 + 3a_3 + 4a_4 + 5a_5 + 4a_6 + 3a_7 + 2a_8 + a_9 + \theta_{t=\infty}^1 + \theta_+^1 + \theta_-^1 = 4F + 2O - 2T,$$

where $a_i = \theta_{t=0}^i$ for $i \in \{1, \dots, 9\}$ and θ_{\pm}^1 denotes the unique component which does not intersect zero in the fibre above $t = \frac{1}{2}(-1 \pm \sqrt{5})$. The set of components $\mathcal{B}_0 = \mathcal{B} \setminus \{\theta_{t=\infty}^1\}$ is a basis of the Néron–Severi group. Indeed, we check by a direct computation based on the intersection graph that the determinant of the sublattice spanned by \mathcal{B}_0 is 24.

We can also replace the generators P and T by $P - O - 2F$ and $T - O - 2F$, respectively, to obtain the following decomposition

$$N = L \oplus U,$$

where L is positive definite of rank 17 and discriminant -24 and U is spanned by F and O and indefinite of rank 2 and discriminant -1 .

Remark 6.3. We checked with `Magma` that the lattice L is not a direct sum of proper sublattices. In the language of [69] and [68], the lattice L is the essential sublattice of N with respect to the given elliptic fibration.

Acknowledgments

The first author is very grateful to Claude Duhr, Lorenzo Tancredi, Robert M. Schabinger, Andreas von Manteuffel, Duco van Straten, and Stefan Weinzierl for lots of helpful discussions. The second author was supported by the grant SFB/TRR 45 in Mainz. The fourth author would like to thank the department of mathematics of Mainz University for the hospitality during his visit in February 2019.

References

- [1] G. Altarelli, R. K. Ellis, M. Greco, and G. Martinelli. Vector Boson Production at Colliders: A Theoretical Reappraisal. *Nucl. Phys.*, B246:12–44, 1984. [4](#)
- [2] G. Altarelli, R. K. Ellis, and G. Martinelli. Large Perturbative Corrections to the Drell-Yan Process in QCD. *Nucl. Phys.*, B157:461–497, 1979. [4](#)
- [3] M. Artin and H. P. F. Swinnerton-Dyer. The Shafarevich-Tate conjecture for pencils of elliptic curves on $K3$ surfaces. *Invent. Math.*, 20:249–266, 1973. [10](#)
- [4] R. Barbieri, J. A. Mignaco, and E. Remiddi. Electron form-factors up to fourth order. - I. *Nuovo Cim.*, A11:824–864, 1972. [6](#)
- [5] W. Barth, K. Hulek, C. Peters, and A. Van de Ven. *Compact Complex Surfaces*, 2nd ed. Springer, 2004. [9](#), [15](#)
- [6] C. W. Bauer, A. Frink, and R. Kreckel. Introduction to the GiNaC framework for symbolic computation within the C++ programming language. *J. Symb. Comput.*, 33:1, 2002. [2](#)
- [7] U. Baur, S. Keller, and W. K. Sakumoto. QED radiative corrections to Z boson production and the forward backward asymmetry at hadron colliders. *Phys. Rev.*, D57:199–215, 1998. [4](#)
- [8] Z. Bern, L. J. Dixon, and D. A. Kosower. Dimensionally regulated pentagon integrals. *Nucl.Phys.*, B412:751–816, 1994. [5](#)
- [9] M. J. Bertin, A. Garbagnati, R. Hortsch, O. Lecacheux, M. Mase, C. Salgado, and U. Whitcher. Classifications of elliptic fibrations of a singular $K3$ surface. In *Women in numbers Europe*, volume 2 of *Assoc. Women Math. Ser.*, pages 17–49. Springer, Cham, 2015. [14](#)
- [10] M. Besier, D. Festi, M. Harrison, and B. Naskręcki. Accompanying MAGMA code. https://bnaskrecki.faculty.wmi.amu.edu.pl/doku.php/drell_yan_k3s, 2019. [3](#), [11](#), [12](#), [16](#), [18](#), [19](#), [20](#)
- [11] M. Besier, D. van Straten, and S. Weinzierl. Rationalizing roots: an algorithmic approach. *Commun. Num. Theor. Phys.*, 13:253–297, 2019. [2](#), [7](#)
- [12] J. Blümlein, A. De Freitas, C. G. Raab, and K. Schönwald. The $O(\alpha^2)$ Initial State QED Corrections to e^+e^- Annihilation to a Neutral Vector Boson Revisited. *Phys. Lett.*, B791:206–209, 2019. [4](#)
- [13] R. Bonciani, S. Di Vita, P. Mastrolia, and U. Schubert. Two-Loop Master Integrals for the mixed EW-QCD virtual corrections to Drell-Yan scattering. *JHEP*, 09:091, 2016. [5](#), [8](#)
- [14] J. Bosma, M. Sogaard, and Y. Zhang. Maximal Cuts in Arbitrary Dimension. *JHEP*, 08:051, 2017. [6](#)
- [15] W. Bosma, J. Cannon, and C. Playoust. The Magma algebra system. I. The user language. *J. Symbolic Comput.*, 24(3-4):235–265, 1997. Computational algebra and number theory (London, 1993). [3](#)
- [16] J. L. Bourjaily, Y.-H. He, A. J. McLeod, M. von Hippel, and M. Wilhelm. Traintracks through Calabi-Yau Manifolds: Scattering Amplitudes beyond Elliptic Polylogarithms. *Phys. Rev. Lett.*, 121(7):071603, 2018. [8](#)
- [17] J. L. Bourjaily, A. J. McLeod, M. von Hippel, and M. Wilhelm. Rationalizing Loop Integration. *JHEP*, 08:184, 2018. [2](#), [7](#)

- [18] J. L. Bourjaily, A. J. McLeod, M. von Hippel, and M. Wilhelm. Bounded Collection of Feynman Integral Calabi-Yau Geometries. *Phys. Rev. Lett.*, 122(3):031601, 2019. [8](#)
- [19] A. P. Braun, Y. Kimura, and T. Watari. On the Classification of Elliptic Fibrations modulo Isomorphism on K3 Surfaces with large Picard Number. arXiv:1312.4421, 2013. [14](#)
- [20] J. Broedel, C. Duhr, F. Dulat, B. Penante, and L. Tancredi. Elliptic polylogarithms and iterated integrals on elliptic curves II: an application to the sunrise integral. *Phys. Rev.*, D97(11):116009, 2018. [13](#)
- [21] J. Broedel, C. Duhr, F. Dulat, and L. Tancredi. Elliptic polylogarithms and iterated integrals on elliptic curves. Part I: general formalism. *JHEP*, 05:093, 2018. [7](#), [13](#)
- [22] F. Brown. On the periods of some Feynman integrals. arXiv:0910.0114, 2009. [8](#)
- [23] F. Brown and A. Levin. Multiple Elliptic Polylogarithms. arXiv:1110.6917, 2011. [7](#)
- [24] F. Brown and O. Schnetz. A K3 in ϕ^4 . *Duke Math. J.*, 161(10):1817–1862, 2012. [8](#)
- [25] S. Caron-Huot, L. J. Dixon, M. von Hippel, A. J. McLeod, and G. Papathanasiou. The Double Pentaladder Integral to All Orders. *JHEP*, 07:170, 2018. [7](#)
- [26] F. Charles. The Tate conjecture for K3 surfaces over finite fields. *Invent. Math.*, 194(1):119–145, 2013. [10](#)
- [27] E. Chaubey and S. Weinzierl. Two-loop master integrals for the mixed QCD-electroweak corrections for $H \rightarrow b\bar{b}$ through a $Ht\bar{t}$ -coupling. *JHEP*, 05:185, 2019. [2](#)
- [28] D. Chicherin, T. Gehrmann, J. M. Henn, P. Wasser, Y. Zhang, and S. Zoia. All master integrals for three-jet production at NNLO. *Phys. Rev. Lett.*, 123:041603, 2019. [6](#)
- [29] G. Cornell and J. H. Silverman. *Arithmetic Geometry*. Springer, 1986. [14](#)
- [30] P. Deligne. La conjecture de Weil pour les surfaces K3. *Invent. Math.*, 15:206–226, 1972. [10](#)
- [31] I. Dolgachev. Weighted projective varieties. In *Group actions and vector fields (Vancouver, B.C., 1981)*, volume 956 of *Lecture Notes in Math.*, pages 34–71. Springer, Berlin, 1982. [2](#)
- [32] S. D. Drell and T.-M. Yan. Massive Lepton Pair Production in Hadron-Hadron Collisions at High-Energies. *Phys. Rev. Lett.*, 25:316–320, 1970. [Erratum: *Phys. Rev. Lett.*25,902(1970)]. [4](#)
- [33] N. D. Elkies. Supersingular primes for elliptic curves over real number fields. *Compositio Math.*, 72(2):165–172, 1989. [26](#)
- [34] D. Festi. A practical algorithm to compute the geometric Picard lattice of K3 surfaces of degree 2. arXiv:1808.00351, 2018. [9](#)
- [35] D. Festi and D. van Straten. Bhabha Scattering and a special pencil of K3 surfaces. *Commun. Num. Theor. Phys.*, 13(2), 2019. [2](#), [3](#), [7](#), [12](#)
- [36] L. R. A. Finotti. A formula for the supersingular polynomial. *Acta Arith.*, 139(3):265–273, 2009. [27](#)
- [37] H. Frellesvig and C. G. Papadopoulos. Cuts of Feynman Integrals in Baikov representation. *JHEP*, 04:083, 2017. [6](#)
- [38] T. Gehrmann, J. M. Henn, and N. A. Lo Presti. Analytic form of the two-loop planar five-gluon all-plus-helicity amplitude in QCD. *Phys. Rev. Lett.*, 116(6):062001, 2016. [Erratum: *Phys. Rev. Lett.*116,no.18,189903(2016)]. [2](#), [7](#)

- [39] T. Gehrmann and E. Remiddi. Differential equations for two loop four point functions. *Nucl.Phys.*, B580:485–518, 2000. [5](#)
- [40] R. Hamberg, W. L. van Neerven, and T. Matsuura. A complete calculation of the order $\alpha - s^2$ correction to the Drell-Yan K factor. *Nucl. Phys.*, B359:343–405, 1991. [Erratum: *Nucl. Phys.*B644,403(2002)]. [4](#)
- [41] M. Harley, F. Moriello, and R. M. Schabinger. Baikov-Lee Representations Of Cut Feynman Integrals. *JHEP*, 06:049, 2017. [6](#)
- [42] R. Hartshorne. *Algebraic Geometry*. Springer, 1977. [14](#), [25](#)
- [43] M. Heller, A. von Manteuffel, and R. M. Schabinger. Multiple polylogarithms with algebraic arguments and the two-loop EW-QCD Drell-Yan master integrals. arXiv:1907.00491, 2019. [2](#), [3](#), [5](#)
- [44] J. M. Henn. Multiloop integrals in dimensional regularization made simple. *Phys. Rev. Lett.*, 110:251601, 2013. [6](#)
- [45] J. M. Henn and V. A. Smirnov. Analytic results for two-loop master integrals for Bhabha scattering I. *JHEP*, 1311:041, 2013. [7](#)
- [46] A. Hodges. Eliminating spurious poles from gauge-theoretic amplitudes. *JHEP*, 05:135, 2013. [7](#)
- [47] D. Huybrechts. *Complex geometry*. Springer, 2005. [28](#)
- [48] D. Huybrechts. *Lectures on K3 surfaces*, volume 158 of *Cambridge Studies in Advanced Mathematics*. Cambridge University Press, 2016. [21](#)
- [49] R. Kloosterman. Elliptic $K3$ surfaces with geometric Mordell-Weil rank 15. *Canad. Math. Bull.*, 50(2):215–226, 2007. [10](#)
- [50] A. V. Kotikov. Differential equations method: New technique for massive Feynman diagrams calculation. *Phys. Lett.*, B254:158–164, 1991. [5](#)
- [51] A. V. Kotikov. The Property of maximal transcendentality in the $\mathcal{N} = 4$ Supersymmetric Yang-Mills. In *Diakonov, D. (ed.): Subtleties in quantum field theory*, pages 150–174, 2010. [6](#)
- [52] A. Kumar and M. Kuwata. Elliptic $K3$ surfaces associated with the product of two elliptic curves: Mordell-Weil lattices and their fields of definition. *Nagoya Math. J.*, 228:124–185, 2017. [22](#)
- [53] S. Laporta and E. Remiddi. Analytic treatment of the two loop equal mass sunrise graph. *Nucl. Phys.*, B704:349–386, 2005. [7](#)
- [54] R. N. Lee and K. T. Mingulov. DREAM, a program for arbitrary-precision computation of dimensional recurrence relations solutions, and its applications. arXiv:1712.05173, 2017. [6](#)
- [55] R. N. Lee and V. A. Smirnov. The Dimensional Recurrence and Analyticity Method for Multicomponent Master Integrals: Using Unitarity Cuts to Construct Homogeneous Solutions. *JHEP*, 12:104, 2012. [6](#)
- [56] T. Matsuura, S. C. van der Marck, and W. L. van Neerven. The Calculation of the Second Order Soft and Virtual Contributions to the Drell-Yan Cross-Section. *Nucl. Phys.*, B319:570–622, 1989. [4](#)
- [57] D. R. Morrison. On $K3$ surfaces with large Picard number. *Invent. Math.*, 75(1):105–121, 1984. [20](#), [21](#)

- [58] B. Naskręcki. Mordell-Weil ranks of families of elliptic curves associated to Pythagorean triples. *Acta Arith.*, 160(2):159–183, 2013. [28](#)
- [59] B. Naskręcki. Distribution of Mordell-Weil ranks of families of elliptic curves. In *Algebra, logic and number theory*, volume 108 of *Banach Center Publ.*, pages 201–229. Polish Acad. Sci. Inst. Math., Warsaw, 2016. [28](#)
- [60] B. Naskręcki. On a certain hypergeometric motive of weight 2 and rank 3. arXiv:1702.07738, 2017. [21](#)
- [61] V. V. Nikulin. Finite groups of automorphisms of Kählerian surfaces of type $K3$. *Uspehi Mat. Nauk*, 31(2(188)):223–224, 1976. [21](#)
- [62] V. V. Nikulin. Elliptic fibrations on $K3$ surfaces. arXiv:1010.3904, 2012. [14](#), [16](#)
- [63] B. Poonen. *Rational points on varieties*, volume 186 of *Graduate Studies in Mathematics*. American Mathematical Society, Providence, RI, 2017. [12](#)
- [64] A. Primo and L. Tancredi. On the maximal cut of Feynman integrals and the solution of their differential equations. *Nucl. Phys.*, B916:94–116, 2017. [6](#)
- [65] I. I. Pyatetskii-Shapiro and I. R. Shafarevich. A Torelli theorem for algebraic surfaces of type $K3$. *Math. USSR Izv.*, 5(3):547–588, 1971. [13](#), [14](#)
- [66] E. Remiddi. Differential equations for Feynman graph amplitudes. *Nuovo Cim.*, A110:1435–1452, 1997. [5](#)
- [67] B. Saint-Donat. Projective Models of $K3$ Surfaces. *Am. J. Math.*, 96(4):602–639, 1974. [14](#)
- [68] M. Schütt and T. Shioda. Elliptic surfaces. In *Algebraic geometry in East Asia—Seoul 2008*, volume 60 of *Adv. Stud. Pure Math.*, pages 51–160. Math. Soc. Japan, Tokyo, 2010. [29](#), [30](#)
- [69] T. Shioda. Mordell-Weil lattices and Galois representation, i. *Proc. Japan Acad. Ser. A Math. Sci.*, 65(7):268–271, 1989. [27](#), [28](#), [29](#), [30](#)
- [70] T. Shioda and H. Inose. On singular $K3$ surfaces. In *Complex Analysis and Algebraic Geometry: A Collection of Papers Dedicated to K. Kodaira*, pages 119–136. Cambridge University Press, 1977. [15](#)
- [71] J. H. Silverman. *The Arithmetic of Elliptic Curves*. Springer, 2nd edition, 1986. [27](#)
- [72] J. H. Silverman. *Advanced topics in the arithmetic of elliptic curves*, volume 151 of *Graduate Texts in Mathematics*. Springer, 1994. [29](#)
- [73] L. Tancredi. Feynman integrals and higher-genus surfaces. Talk at Amplitudes Conference, 2019. [3](#), [8](#), [13](#)
- [74] J. Tate. Algorithm for determining the type of a singular fiber in an elliptic pencil. *Lecture Notes in Math., Vol. 476*, pages 33–52, 1975. [29](#)
- [75] R. van Luijk. $K3$ surfaces with Picard number one and infinitely many rational points. *Algebra Number Theory*, 1(1):1–15, 2007. [10](#), [28](#)
- [76] J. Vollinga and S. Weinzierl. Numerical evaluation of multiple polylogarithms. *Comput. Phys. Commun.*, 167:177, 2005. [2](#)
- [77] A. von Manteuffel and R. M. Schabinger. Numerical Multi-Loop Calculations via Finite Integrals and One-Mass EW-QCD Drell-Yan Master Integrals. *JHEP*, 04:129, 2017. [5](#)
- [78] A. von Manteuffel and L. Tancredi. A non-planar two-loop three-point function beyond multiple polylogarithms. *JHEP*, 06:127, 2017. [2](#)

- [79] D. Wackerth and W. Hollik. Electroweak radiative corrections to resonant charged gauge boson production. *Phys. Rev.*, D55:6788–6818, 1997. [4](#)